

# Anti-inflammatory Quinoline Alkaloids from the Roots of *Waltheria indica*

Feifei Liu, Timothy J. O'Donnell, Eun-Jung Park, Sasha Kovacs, Kenzo Nakamura, Asim Dave, Yuheng Luo, Rui Sun, Marisa Wall, Supakit Wongwiwatthanakit, Dane Kaohelani Silva, Philip G. Williams, John M. Pezzuto, and Leng Chee Chang\*



Cite This: *J. Nat. Prod.* 2023, 86, 276–289



Read Online

ACCESS |



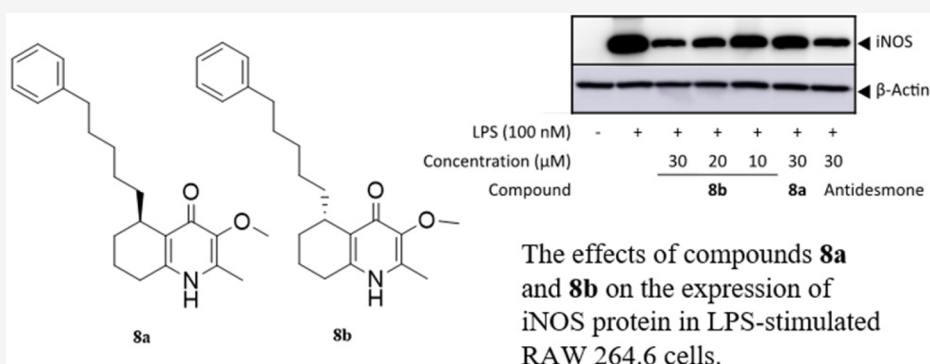
Metrics & More



Article Recommendations



Supporting Information



**ABSTRACT:** Sixteen new quinoline alkaloids (**1a–7**, **8a**, **9**, **10**, **13–15**, **17**, and **21**) and 10 known analogs (**8b**, **11**, **12**, **16**, **18–20**, and **22–24**), along with three known cyclopeptide alkaloids (**25–27**), were isolated from the roots of *Waltheria indica*. The structures of the new compounds were elucidated by detailed NMR and circular dichroism with computational support and mass spectrometry data interpretation. Anti-inflammatory potential of isolates was evaluated based on inhibition of lipopolysaccharide (LPS)-induced nitric oxide (NO) production and tumor necrosis factor- $\alpha$  (TNF- $\alpha$ )-induced nuclear factor kappa B (NF- $\kappa$ B) activity with cell culture models. In the absence of cell growth inhibition, compounds **6**, **8a**, **9–11**, **13**, **21**, and **24** reduced TNF- $\alpha$ -induced NF- $\kappa$ B activity with IC<sub>50</sub> values ranging from 7.1 to 12.1  $\mu$ M, comparable to the positive control (BAY 11-7082, IC<sub>50</sub> = 9.7  $\mu$ M). Compounds **6**, **8a**, **8b**, and **11** showed significant NO-inhibitory activity with IC<sub>50</sub> values ranging from 11.0 to 12.8  $\mu$ M, being more active than the positive control (L-NMMA, IC<sub>50</sub> = 22.7  $\mu$ M). Structure–activity relationships indicated that NO inhibitory activity was significantly affected by C-8 substitution. Inhibition of LPS-induced nitric oxide synthase (iNOS) by **8b** [(*SS*)-waltherione M, IC<sub>50</sub> 11.7  $\pm$  0.8  $\mu$ M] correlated with inhibition of iNOS mRNA expression. The biological potential of *W. indica* metabolites supports the traditional use of this plant for the treatment of inflammatory-related disorders.

Inflammation is a complex defense process caused by many factors, such as physical damage, chemical stimulus, and bacterial infections. However, excessive inflammation may contribute to the genesis of acute and chronic diseases, including hepatitis, arthritis, encephalitis, multiple sclerosis, and cancer.<sup>2,3</sup> Currently, nonsteroidal anti-inflammatory drugs and synthetic forms of natural cortisol (termed glucocorticoids) are widely used to treat inflammatory diseases, and despite their side effects, they remain a mainstay for reducing inflammation.<sup>4</sup> Thus, the goal of developing more effective and less toxic agents to treat inflammation-related diseases remains a significant challenge.

Since ancient times, plants or plant-derived formulations have been employed for the improvement of inflammatory conditions and associated disorders. An example is *Waltheria indica* (Malvaceae), also known as ‘uhaloa or *Waltheria indica* var. *americana* in Hawaii.<sup>5,6</sup> In Hawaiian traditional medicinal

practices, ‘uhaloa is one of the most highly recognized plants for treating inflammatory-related disorders.<sup>5,7</sup> Of relevance, previous investigations have demonstrated extracts of *W. indica* inhibit the expression of key inflammatory cytokines and cytokine receptors, reduce mRNA and protein levels of TNF- $\alpha$ , inhibit TNF- $\alpha$ -associated pro-inflammatory signaling, together with significant reduction of NF- $\kappa$ B mRNA and protein, and diminish activities of multiple pro-inflammatory signaling pathways.<sup>6</sup> However, despite evidence suggesting the

Received: September 25, 2022

Published: February 6, 2023



Table 1.  $^{13}\text{C}$  NMR (100 MHz) Data for Compounds 1a–7 and 8a ( $\delta_{\text{C}}$  in ppm, type)

position	1a <sup>a</sup>	1b <sup>a</sup>	2 <sup>a</sup>	3 <sup>a</sup>	4 <sup>a</sup>	5 <sup>b</sup>	6 <sup>b</sup>	7 <sup>a</sup>	8a <sup>a</sup>
2	144.4, C	144.4, C	145.3, C	143.0, C	142.8, C	139.8, C	139.8, C	145.3, C	140.3, C
3	143.7, C	143.7, C	142.7, C	143.4, C	143.1, C	140.9, C	140.6, C	142.7, C	145.9, C
4	175.0, C	175.0, C	173.0, C	176.1, C	176.2, C	173.1, C	173.2, C	173.0, C	174.7, C
5	137.1, C	137.1, C	131.0, C	136.8, C	135.7, C	133.2, C	144.0, C	130.9, C	32.5, CH
6	124.4, CH	124.3, CH	121.9, CH	125.6, CH	125.8, CH	123.5, CH	124.0, CH	122.0, CH	26.0, CH <sub>2</sub>
7	110.5, CH	110.5, CH	110.6, CH	110.8, CH	114.2, CH	112.7, CH	130.0, CH	110.5, CH	18.2, CH <sub>2</sub>
8	149.4, C	149.4, C	150.7, C	148.1, C	145.6, C	144.2, C	116.0, CH	150.7, C	27.7, CH <sub>2</sub>
9	132.9, C	132.9, C	135.0, C	132.6, C	132.2, C	130.4, C	140.2, C	134.9, C	144.6, C
10	125.0, C	125.0, C	125.1, C	125.2, C	125.4, C	123.9, C	123.0, C	125.0, C	129.6, C
11	77.0, CH	77.0, CH	211.3, C	36.4, CH <sub>2</sub>	36.5, CH <sub>2</sub>	34.4, CH <sub>2</sub>	34.8, CH <sub>2</sub>	211.1, C	33.7, CH <sub>2</sub>
12	39.3, CH <sub>2</sub>	39.3, CH <sub>2</sub>	45.9, CH <sub>2</sub>	33.6, CH <sub>2</sub>	34.0, CH <sub>2</sub>	32.0, CH <sub>2</sub>	31.7, CH <sub>2</sub>	45.7, CH <sub>2</sub>	28.9, CH <sub>2</sub>
13	27.9, CH <sub>2</sub>	27.9, CH <sub>2</sub>	25.8, CH <sub>2</sub>	30.7, CH <sub>2</sub>	31.1, CH <sub>2</sub>	28.7, CH <sub>2</sub>	28.5, CH <sub>2</sub>	25.4, CH <sub>2</sub>	30.7, CH <sub>2</sub>
14	30.8, CH <sub>2</sub>	30.8, CH <sub>2</sub>	30.5, CH <sub>2</sub>	30.4, CH <sub>2</sub>	31.0, CH <sub>2</sub>	31.2, CH <sub>2</sub>	31.1, CH <sub>2</sub>	32.4, CH <sub>2</sub>	33.0, CH <sub>2</sub>
15	30.5, CH <sub>2</sub>	30.6, CH <sub>2</sub>	30.5, CH <sub>2</sub>	25.1, CH <sub>2</sub>	30.7, CH <sub>2</sub>	35.2, CH <sub>2</sub>	35.2, CH <sub>2</sub>	36.9, CH <sub>2</sub>	37.1, CH <sub>2</sub>
16	33.1, CH <sub>2</sub>	33.1, CH <sub>2</sub>	33.1, CH <sub>2</sub>	44.5, CH <sub>2</sub>	33.2, CH <sub>2</sub>	142.5, C	142.5, C	143.8, C	144.2, C
17	23.8, CH <sub>2</sub>	23.9, CH <sub>2</sub>	23.8, CH <sub>2</sub>	212.5, C	23.9, CH <sub>2</sub>	128.3, CH	128.3, CH	129.6, CH	129.5, CH
18	14.6, CH <sub>3</sub>	14.6, CH <sub>3</sub>	14.6, CH <sub>3</sub>	22.9, CH <sub>3</sub>	14.6, CH <sub>3</sub>	128.2, CH	128.2, CH	129.4, CH	129.4, CH
19						125.5, CH	125.5, CH	126.7, CH	126.7, CH
20						128.2, CH	128.2, CH	129.4, CH	129.4, CH
21						128.3, CH	128.3, CH	129.6, CH	129.5, CH
CH <sub>3</sub> -2	14.3, CH <sub>3</sub>	14.3, CH <sub>3</sub>	14.4, CH <sub>3</sub>	14.3, CH <sub>3</sub>	14.3, CH <sub>3</sub>	13.8, CH <sub>3</sub>	14.0, CH <sub>3</sub>	14.4, CH <sub>3</sub>	13.7, CH <sub>3</sub>
OCH <sub>3</sub> -3	60.4, CH <sub>3</sub>	60.4, CH <sub>3</sub>	60.5, CH <sub>3</sub>	60.4, CH <sub>3</sub>	60.4, CH <sub>3</sub>	58.6, CH <sub>3</sub>	58.8, CH <sub>3</sub>	60.5, CH <sub>3</sub>	60.3, CH <sub>3</sub>
OCH <sub>3</sub> -8	56.9, CH <sub>3</sub>	56.9, CH <sub>3</sub>	57.1, CH <sub>3</sub>	56.7, CH <sub>3</sub>				57.1, CH <sub>3</sub>	

<sup>a</sup>Compounds 1a, 1b, 2, 3, 4, 7, and 8a were determined in MeOD. <sup>b</sup>Compounds 5 and 6 were determined in DMSO-*d*<sub>6</sub>.

anti-inflammatory potential of *W. indica*, there is limited knowledge regarding the bioactive constituents responsible for these effects. We herein report the isolation and structural characterization of 29 compounds, including 16 new quinoline alkaloids, from a Hawaiian sample of *W. indica*, along with anti-inflammatory activity determined with model systems.

## RESULTS AND DISCUSSION

The powdered roots of *W. indica* were extracted with MeOH at room temperature and then successively extracted with *n*-hexane and EtOAc. The EtOAc-soluble partition was fractionated on an MCI gel CHP-20P column. Further purifications of the fractions were carried out by a series of chromatographic procedures and yielded 16 new compounds, namely, 1a–7, 8a, 9, 10, 13–15, 17, and 21, as well as waltherione M (8b),<sup>8</sup> waltherione G (11),<sup>9</sup> waltherione H (12),<sup>9</sup> waltherione P (16),<sup>8</sup> antidesmone (18),<sup>10</sup> 8-deoxoantidesmone (19),<sup>11</sup> waltherione E (20),<sup>8</sup> waltherione A (22),<sup>12</sup> waltherione E2 (23),<sup>13</sup> waltherione C (24),<sup>14</sup> scutianene L (25),<sup>15</sup> adouetin Y (26),<sup>16</sup> and amaouiine (27).<sup>17</sup> Electrospray ionization mass spectrometry (ESIMS) analysis of compounds 1a–24 suggested the presence of a nitrogen atom in their molecular formula. Analysis of UV data, NMR data (Tables 1–4), 2D NMR experiments, and comparison with the literature, suggested a quinoline alkaloid skeleton for this series of compounds.<sup>8,9</sup>

Compound 1 was obtained as a pale-yellow oil. Its molecular formula of C<sub>20</sub>H<sub>29</sub>NO<sub>4</sub> was proposed based on the HRESIMS (*m/z* 348.2172 [M + H]<sup>+</sup>) and  $^{13}\text{C}$  NMR data (Table 1), with seven degrees of unsaturation. The IR spectrum suggested the presence of hydroxyl group (3300 cm<sup>-1</sup>) and aromatic ring (1626 and 1524 cm<sup>-1</sup>) functionalities. Analysis of HSQC and HMBC spectra indicated the presence of three *sp*<sup>2</sup> carbons linked to a nitrogen atom at  $\delta_{\text{C}}$  144.4, 143.7, and 132.9 (C-2, C-3, and C-9, respectively), three quaternary aromatic carbons

at  $\delta_{\text{C}}$  137.1, 149.4, and 125.0 (C-5, C-8, and C-10, respectively), two aromatic methines at  $\delta_{\text{C}}$  124.4 and 110.5 (C-6 and C-7, respectively), two methoxy groups at  $\delta_{\text{C}}$  60.4 and 56.9 (MeO-3 and MeO-8, respectively), six methylenes at  $\delta_{\text{C}}$  39.3, 33.1, 30.8, 30.5, 27.9, and 23.8 (C-12–C-17, respectively), one oxymethine at  $\delta_{\text{C}}$  77.0 (C-11), and two methyl groups at  $\delta_{\text{C}}$  14.3 and 14.6 (Me-2 and C-18, respectively). The spectroscopic data of 1 were closely related to those of 3,8-dimethoxy-2-methyl-5-octylquinolin-4(1*H*)-one (waltherione F),<sup>9</sup> previously isolated from the same plant. Compared to waltherione F, the molecular formula of 1 differed from waltherione F by 16 mass units, which can be accounted for by the absence of a methylene ( $\delta_{\text{H}}$  3.27, m, H-11, 2H;  $\delta_{\text{C}}$  36.4, C-11) in waltherione F that was replaced by an oxymethine ( $\delta_{\text{H}}$  4.96, dd, H-11, 1H;  $\delta_{\text{C}}$  77.0, C-11) in 1. Thus, 1 is the 11-hydroxyl derivative of waltherione F. Further confirmation of this supposition was provided by the correlations of H-11 ( $\delta_{\text{H}}$  4.96) with C-5 ( $\delta_{\text{C}}$  137.1), C-6 ( $\delta_{\text{C}}$  124.4), and C-10 ( $\delta_{\text{C}}$  125.0) in the HMBC spectrum (Figure 1). Compound 1 was thus identified as 11-hydroxy-waltherione F. The optical rotation of 1 was approximately zero, and the circular dichroism (CD) spectrum showed no significant Cotton effects, which indicated that the compound was isolated as a scalemic mixture. Further analysis by HPLC using a chiral-phase column showed two peaks (*t*<sub>R</sub> = 21.4 and 23.2 min) with areas in an approximately 10:11 ratio, and their CD spectra were nearly mirror images (Figure 2). The absolute configurations of the faster eluting enantiomer and the slower eluting enantiomer were assigned as 11R (1a) and 11S (1b), respectively, based on ECD calculations. The similarity score calculated for 1a was 0.5980 with the enantiomer as 0.0009 and, for 1b, was 0.5889 with the enantiomer as 0.0001 with  $\sigma$  = 0.3 and a +30 nm shift as calculated by SpecDis.<sup>18</sup> The wavelength shift was justified after reviewing the HOMO to LUMO orbitals (visualized using Multiwfn software), which

Table 2. <sup>1</sup>H NMR (400 MHz) Data for Compounds 1a–7 and 8a (δ<sub>C</sub> in ppm, J in Hz)

position	1a <sup>a</sup>	1b <sup>a</sup>	2 <sup>a</sup>	3 <sup>a</sup>	4 <sup>a</sup>	5 <sup>b</sup>	6 <sup>b</sup>	7 <sup>a</sup>	8a <sup>a</sup>
5									2.90, (m)
6	7.24, d (8.3)	7.25, d (8.2)	6.98, d (8.0)	6.94, d (8.4)	6.80, d (8.0)	6.69, d (8.0)	6.89, d (7.0)	6.95, d (8.0)	1.53, (m) 1.90, (m)
7	7.12, d (8.3)	7.12, d (8.2)	7.17, d (8.0)	7.03, d (8.4)	6.88, d (8.0)	6.84, d (8.0)	7.38, dd (7.0, 8.4)	7.14, d (8.0)	1.76, (m)
8							7.31, d (8.4)		2.59, (m)
11	4.96, dd (5.7, 7.1)	4.97, dd (5.7, 7.5)		3.26, t (7.6)	3.23, t (7.7)	3.15, t (7.5)	3.27, t (7.7)		1.25, (m) 1.72, (m)
12	1.76, (m) 1.87, (m)	1.76, (m) 1.87, (m)	2.73, d (7.5)	1.59, (m)	1.58, (m)	1.49, (m)	1.55, (m)	2.77, t (7.4)	1.45, (m)
13	1.29, (m) 1.48, (m)	1.29, (m) 1.48, (m)	1.71, (m)	1.35, (m)	1.28, (m)	1.32, (m)	1.35, (m)	1.73, (m)	1.35, (m)
14	1.26, (m)	1.26, (m)	1.31, (m)	1.33, (m)	1.28, (m)	1.58, (m)	1.58, (m)	1.67, (m)	1.64, (m)
15	1.28, (m)	1.28, (m)	1.31, (m)	1.55, (m)	1.28, (m)	2.55, t (7.7)	2.55, t (7.7)	2.61, t (7.4)	2.59, t (7.6)
16	1.26, (m)	1.26, (m)	1.28, (m)	2.46, t (7.2)	1.26, (m)				
17	1.28, (m)	1.28, (m)	1.29, (m)		1.28, (m)	7.17, d (7.0)	7.25, d (7.4)	7.14, d (7.4)	7.22, d (7.3)
18	0.85, t (7.1)	0.87, t (7.1)	0.87, t (7.1)	2.12, (s)	0.88, t (6.8)	7.24, t (7.0)	7.18, t (7.4)	7.21, t (7.4)	7.16, t (7.3)
19						7.14, t (7.0)	7.17, t (7.4)	7.11, t (7.4)	7.12, t (7.3)
20						7.24, t (7.0)	7.18, t (7.4)	7.21, t (7.4)	7.16, t (7.3)
21						7.17, d (7.0)	7.25, d (7.4)	7.14, d (7.4)	7.22, d (7.3)
CH <sub>3</sub> -2	2.55, (s)	2.55, (s)	2.52, (s)	2.48, (s)	2.47, (s)	2.37, (s)	2.32, (s)	2.52, (s)	2.28, (s)
OCH <sub>3</sub> -3	3.81, (s)	3.81, (s)	3.79, (s)	3.78, (s)	3.77, (s)	3.67, (s)	3.68, (s)	3.78, (s)	3.74, (s)
OCH <sub>3</sub> -8	4.05, (s)	4.05, (s)	4.06, (s)	4.00, (s)				4.06, (s)	
OH-8						10.38, (s)			

<sup>a</sup>Compounds 1a, 1b, 2, 3, 4, 7, and 8a were measured in MeOD. <sup>b</sup>Compounds 5 and 6 were measured in DMSO-*d*<sub>6</sub>.

Table 3.  $^{13}\text{C}$  NMR (100 MHz) Data for Compounds 9, 10, 13–15, 17, and 21 ( $\delta_{\text{C}}$  in ppm, Type)<sup>a</sup>

position	9	10	13	14	15	17	21
2	141.1, C	141.1, C	147.2, C	143.2, C	143.2, C	147.2, C	143.6, C
3	145.5, C	145.6, C	144.1, C	149.1, C	149.1, C	144.0, C	143.0, C
4	172.8, C	172.9, C	174.7, C	<sup>b</sup>	174.5, C	174.8, C	175.8, C
5	32.8, CH	32.6, CH	32.1, CH	32.1, CH	31.9, CH	32.1, CH	144.3, C
6	25.5, CH <sub>2</sub>	25.7, CH <sub>2</sub>	25.5, CH <sub>2</sub>	25.4, CH <sub>2</sub>	25.4, CH <sub>2</sub>	25.5, CH <sub>2</sub>	130.6, C
7	18.0, CH <sub>2</sub>	17.7, CH <sub>2</sub>	33.3, CH <sub>2</sub>	33.6, CH <sub>2</sub>	33.6, CH <sub>2</sub>	33.3, CH <sub>2</sub>	134.2, CH
8	24.6, CH <sub>2</sub>	24.4, CH <sub>2</sub>	195.3, C	195.2, C	195.2, C	195.2, C	117.7, CH
9	145.1, C	145.2, C	134.2, C	135.0, C	135.1, C	134.1, C	139.5, C
10	129.9, C	129.7, C	140.2, C	139.9, C	139.7, C	140.3, C	122.2, C
11	33.5, CH <sub>2</sub>	33.2, CH <sub>2</sub>	29.4, CH <sub>2</sub>	29.4, CH <sub>2</sub>	31.6, CH <sub>2</sub>	31.9, CH <sub>2</sub>	45.9, CH
12	29.0, CH <sub>2</sub>	28.6, CH <sub>2</sub>	31.8, CH <sub>2</sub>	31.9, CH <sub>2</sub>	29.0, CH <sub>2</sub>	29.6, CH <sub>2</sub>	73.0, CH
13	30.6, CH <sub>2</sub>	25.7, CH <sub>2</sub>	30.5, CH <sub>2</sub>	30.4, CH <sub>2</sub>	25.6, CH <sub>2</sub>	30.9, CH <sub>2</sub>	24.9, CH <sub>2</sub>
14	33.2, CH <sub>2</sub>	39.6, CH <sub>2</sub>	32.8, CH <sub>2</sub>	33.0, CH <sub>2</sub>	39.4, CH <sub>2</sub>	30.6, CH <sub>2</sub>	36.3, CH <sub>2</sub>
15	36.2, CH <sub>2</sub>	203.2, C	37.0, CH <sub>2</sub>	36.2, CH <sub>2</sub>	203.0, C	31.0, CH <sub>2</sub>	77.2, CH
16	135.0, C	138.5, C	144.1, C	135.0, C	138.5, C	33.2, CH <sub>2</sub>	
17	130.4, CH	129.4, CH	129.6, CH	130.4, CH	129.4, CH	23.9, CH <sub>2</sub>	
18	116.1, CH	129.9, CH	129.4, CH	116.1, CH	129.9, CH	14.6, CH <sub>3</sub>	
19	156.3, C	134.3, CH	126.8, CH	156.4, C	134.4, CH		
20	116.1, CH	129.9, CH	129.4, CH	116.1, CH	129.9, CH		
21	130.4, CH	129.4, CH	129.6, CH	130.4, CH	129.4, CH		
OCH <sub>3</sub> -1	66.3, CH <sub>3</sub>	66.4, CH <sub>3</sub>					
CH <sub>3</sub> -2	10.5, CH <sub>3</sub>	10.5, CH <sub>3</sub>		13.8, CH <sub>3</sub>	13.8, CH <sub>3</sub>		14.4, CH <sub>3</sub>
CH <sub>2</sub> OH-2			56.9, CH <sub>2</sub>			56.9, CH <sub>2</sub>	
OCH <sub>3</sub> -3	60.4, CH <sub>3</sub>	60.4, CH <sub>3</sub>	60.3, CH <sub>3</sub>	60.0, CH <sub>3</sub>	60.8, CH <sub>3</sub>	60.2, CH <sub>3</sub>	60.5, CH <sub>3</sub>
1'							129.6, C
2'							160.0, C
3'							111.7, CH
4'							129.4, CH
5'							121.4, CH
6'							130.5, CH
OCH <sub>3</sub> -2'							56.1, CH <sub>3</sub>

<sup>a</sup>Compounds 9, 10, 13–15, 17, and 21 were measured in MeOD. <sup>b</sup>Signal too weak to be observed.

are dominated by a  $\pi \rightarrow \pi^*$  transition of extended conjugation across the two ring systems.<sup>19</sup> Despite the difference in ring systems, these spectra resemble the Cotton effects observed in the calculated and experimental spectra of waltheriones G, I, and J, where G and J are both *S* and I is *R*.<sup>9</sup> The major difference is the dichroic peaks here exhibit the expected bathochromic shift due to the extended conjugation. The distortions in the experimental ECD spectra likely arise from the known hydroxypyridine–pyridone tautomerism.<sup>10</sup>

The molecular formulas of compounds 2 (C<sub>20</sub>H<sub>27</sub>NO<sub>4</sub>), 3 (C<sub>20</sub>H<sub>27</sub>NO<sub>4</sub>), and 4 (C<sub>19</sub>H<sub>27</sub>NO<sub>3</sub>) were established on the basis of HRESIMS and  $^{13}\text{C}$  NMR data, respectively. The UV, IR, and NMR spectroscopic data (Tables 1 and 2) of compounds 2–4 also closely resembled those of waltherione F<sup>9</sup> and 1, suggesting these three compounds are homologues of one another. An additional oxygen atom minus two hydrogen atoms was evident for 2 and 3; a carbon atom and two hydrogen atoms were reduced for 4. The differences could be explained by inspection of the HMBC spectra, where the H-6 ( $\delta_{\text{H}}$  6.98) and the H-12 ( $\delta_{\text{H}}$  2.73) signals correlated with a carbonyl at  $\delta_{\text{C}}$  211.3 (C-11) in 2; the H-16 ( $\delta_{\text{H}}$  2.46) and the H-18 ( $\delta_{\text{H}}$  2.12) signals correlated with a carbonyl at  $\delta_{\text{C}}$  212.5 (C-17) in 3; and the absence of signals between OCH<sub>3</sub>-8 and C-8 ( $\delta_{\text{C}}$  145.6) in 4. Therefore, the structures of 2–4 could be assigned as 3,8-dimethoxy-2-methyl-5-octanoylquinolin-4(1*H*)-one, 3,8-dimethoxy-2-methyl-5-(7-oxooctyl)quinolin-

4(1*H*)-one, and 8-hydroxy-3-methoxy-2-methyl-5-octylquinolin-4(1*H*)-one, respectively, named as walindicaones A–C.

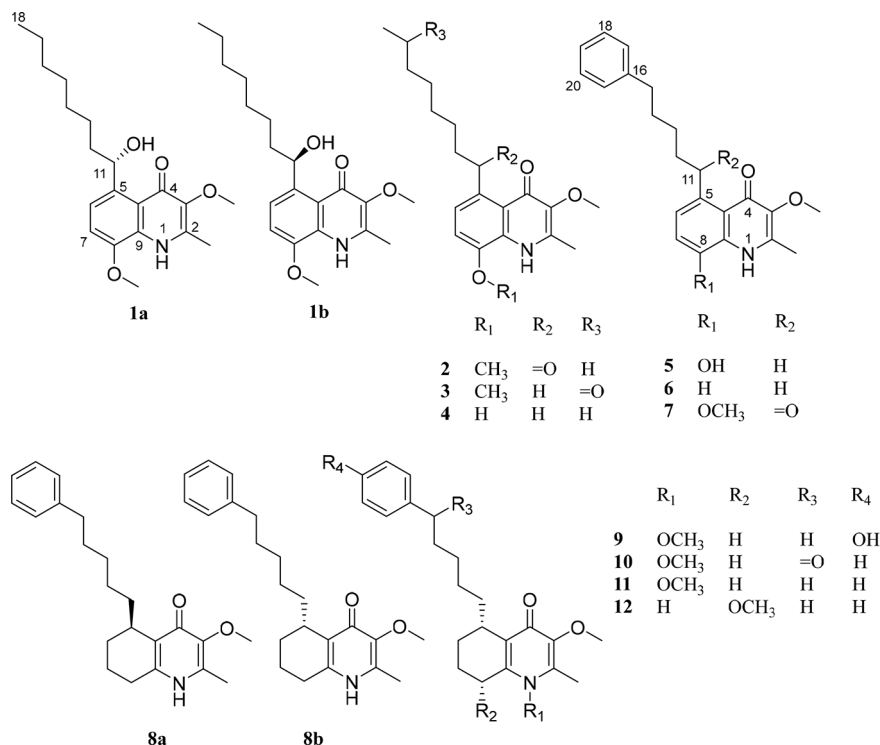
The molecular formulas of compounds 5 (C<sub>22</sub>H<sub>25</sub>NO<sub>3</sub>), 6 (C<sub>22</sub>H<sub>25</sub>NO<sub>2</sub>), and 7 (C<sub>23</sub>H<sub>25</sub>NO<sub>4</sub>) were established on the basis of HRESIMS and  $^{13}\text{C}$  NMR data, respectively. When compared to those of 1–4, the NMR data of 5–7 indicated five aromatic protons at  $\delta_{\text{H}}$  7.11–7.25 in the terminal position of the *n*-pentyl chain, instead of the *n*-terminal methyl group (H-18) signals in 1–4. Detailed NMR analysis revealed that compounds 5–7 were closely related to waltherione R.<sup>20</sup> Compared to waltherione R, the methoxy (OCH<sub>3</sub>-8) in waltherione R ( $\delta_{\text{H}}$  4.00, s, 3H;  $\delta_{\text{C}}$  56.3) was replaced by a hydroxy group ( $\delta_{\text{H}}$  10.38, s, OH-8) in 5 and by an aromatic proton ( $\delta_{\text{H}}$  7.31, d, H-8) in 6, and the CH<sub>2</sub>-11 methylene in waltherione R ( $\delta_{\text{H}}$  3.27, m, 2H;  $\delta_{\text{C}}$  36.0) was replaced by a carbonyl group ( $\delta_{\text{C}}$  211.1, C-11) in 7. These assignments were respectively supported by the HMBC correlation signals from OH-8 to C-7 ( $\delta_{\text{C}}$  112.7) and C-9 ( $\delta_{\text{C}}$  130.4) in 5; the HMBC correlations from H-8 to C-6 ( $\delta_{\text{C}}$  124.0) and C-10 ( $\delta_{\text{C}}$  123.0) in conjunction with  $^1\text{H}$ – $^1\text{H}$  COSY correlation between H-7 ( $\delta_{\text{H}}$  7.38, dd, H-7) and H-8 in 6; and the HMBC correlations from H-6 ( $\delta_{\text{H}}$  6.95, d, H-6) and H-12 ( $\delta_{\text{H}}$  2.77, t, H-12) to C-11 in 7. Therefore, the structures of 5–7 were assigned as 8-hydroxy-3-methoxy-2-methyl-5-(5-phenylpentyl)quinolin-4(1*H*)-one (walindicaone D), 3-methoxy-2-methyl-5-(5-phenylpentyl)-quinolin-4(1*H*)-one (8-demethoxywaltherione R),

Table 4. <sup>1</sup>H NMR (400 MHz) Data for Compounds 9, 10, 13–15, 17, and 21 ( $\delta_C$  in ppm, *J* in Hz)<sup>a</sup>

position	9	10	13	14	15	17	21
5	2.94, (m)	2.98, (m)	3.19, (m)	3.19, (m)	3.22, (m)	3.20, (m)	
6	1.53, (m)	1.46, (m)	2.11, (m)	2.09, (m)	2.09, (m)	2.12, (m)	
	1.91, (m)	1.94, (m)	2.22, (m)	2.20, (m)	2.22, (m)	2.24, (m)	
7	1.84, (m)	1.87, (m)	2.57, ddd (2.6, 4.1, 18.6)	2.53, ddd (2.6, 4.1, 18.6)	2.54, ddd (2.6, 4.4, 18.1)	2.57, ddd (2.4, 4.3, 18.4)	7.14, d (8.7)
8	2.74, (m)	2.75, (m)	2.84, ddd (5.0, 14.6, 18.6)	2.80, ddd (5.0, 14.7, 18.6)	2.84, ddd (5.5, 14.8, 18.1)	2.85, ddd (5.4, 15.0, 18.4)	7.30, d (8.7)
	3.01, (m)	3.02, (m)					
11	1.24, (m)	1.35, (m)	1.37, (m)	1.52, (m)	1.63, (m)	1.55, (m)	5.29, d (5.5)
	1.71, (m)	1.80, (m)	1.59, (m)	1.52, (m)	1.78, (m)	1.70, (m)	
12	1.45, (m)	1.57, (m)	1.56, (m)	1.52, (m)	1.67, (m)	1.56, (m)	4.80, d (6.1)
			1.72, (m)	1.69, (m)	1.80, (m)		
13	1.34, (m)	1.78, (m)	1.43, (m)	1.39, (m)	1.78, (m)	1.34, (m)	1.65, (m)
							1.87, (m)
14	1.58, (m)	3.07, (m)	1.67, (m)	1.61, (m)	3.10, (m)	1.34, (m)	2.19, (m)
15	2.50, t (7.6)		2.61, t (7.6)	2.52, t (7.6)		1.34, (m)	2.36, (m)
16						1.30, (m)	6.61, d (6.8)
17	6.97, d (8.4)	8.00, d (7.4)	7.16, d (7.2)	6.98, d (8.5)	8.00, d (7.4)	1.31, (m)	
18	6.67, d (8.4)	7.49, t (7.4)	7.23, t (7.2)	6.67, d (8.5)	7.49, t (7.4)	0.91, t (7.0)	
19		7.59, t (7.4)	7.12, t (7.2)		7.59, t (7.4)		
20	6.67, d (8.4)	7.49, t (7.4)	7.23, t (7.2)	6.67, d (8.5)	7.49, t (7.4)		
21	6.97, d (8.4)	8.00, d (7.4)	7.16, d (7.2)	6.98, d (8.5)	8.00, d (7.4)		
OCH <sub>3</sub> -1	3.98, (s)	3.99, (s)					2.45, (s)
CH <sub>3</sub> -2	2.46, (s)	2.46, (s)		2.39, (s)	2.39, (s)	4.74, (s)	
CH <sub>2</sub> OH-2			4.74, (s)			3.87, (s)	
OCH <sub>3</sub> -3	3.77, (s)	3.77, (s)	3.86, (s)	3.82, (s)	3.82, (s)		3.81, (s)
3'							7.02, d (8.6)
4'							7.24, dd (8.6, 8.6)
5'							6.82, dd (8.6, 8.6)
6'							6.71, d (8.6)
OCH <sub>3</sub> -2'							3.92, (s)

<sup>a</sup>Compounds 9, 10, 13–15, 17, and 21 were measured in MeOD.

Chart 1



and 3,8-dimethoxy-2-methyl-5-(5-phenylpentanoyl)quinolin-4(1*H*)-one (walindicaone E), respectively.

The <sup>1</sup>H and <sup>13</sup>C NMR spectra of compound **8** are nearly the same as waltherione M.<sup>8</sup> Analysis of 2D NMR data revealed that compound **8** had an identical planar structure to that of waltherione M. The optical rotation of **8** was approximately zero, and the CD spectrum showed no strong signals, which proved that the compound was isolated as a scalemic mixture. Analysis by HPLC using a chiral-phase column showed two peaks (*t<sub>R</sub>* = 21.4 and 23.2 min) with areas in an approximately 4:5 ratio for **8a**/**8b**. CD spectra of isolated enantiomers were nearly mirror images (Figure 3). Their absolute configuration at C-5 was established by comparison with the experimental ECD spectrum of previously published data for waltheriones G, I, J, M, and O.<sup>8,9</sup> The experimental ECD spectrum of the faster eluting enantiomer **8a** exhibited negative and positive Cotton effects (CEs) at 258 and 286 nm, respectively, similar to waltheriones I and O (calcd *SR*);<sup>8,9</sup> the slower eluting enantiomer **8b** exhibited positive and negative CEs at 258 and 286 nm, respectively, similar to waltheriones G, J, and M (calcd *SS*).<sup>8,9</sup> Thus, the structures of **8a** and **8b** were identified as (*SR*)-waltherione M and (*SS*)-waltherione M, respectively.

The molecular formulas of compounds **9** (C<sub>23</sub>H<sub>31</sub>NO<sub>4</sub>) and **10** (C<sub>23</sub>H<sub>29</sub>NO<sub>4</sub>) were established on the basis of HRESIMS and <sup>13</sup>C NMR data, respectively. The <sup>1</sup>H and <sup>13</sup>C NMR spectra of **9** and **10** were closely related to those of waltherione G (**11**).<sup>8</sup> Analysis of the HSQC and HMBC data revealed that a hydrogen atom ( $\delta_{\text{H}}$  7.13, t, H-19) was replaced by a hydroxy group (OH-19) in **9** and a methylene ( $\delta_{\text{H}}$  2.60, t, 2H;  $\delta_{\text{C}}$  36.9, CH<sub>2</sub>-15) was replaced by a carbonyl group ( $\delta_{\text{C}}$  203.2, C-15) in **10**. The ECD spectra of alkaloids **9** and **10** were almost identical to that of **8b**, with a positive CE at 260 nm and a negative CE at 290 nm. Thus, their absolute configuration at C-5 was established as *S* for both. Alkaloids **9** and **10** were identified as 1,3-dimethoxy-2-methyl-5-[5-(4-hydroxyphenyl)-

pentyl]-5,6,7,8-tetrahydroquinolin-4(1*H*)-one (walindicaone F) and 1,3-dimethoxy-2-methyl-5-(5-oxo-5-phenylpentyl)-5,6,7,8-tetrahydroquinolin-4(1*H*)-one (walindicaone G), respectively.

The molecular formulas of compounds **13** (C<sub>22</sub>H<sub>27</sub>NO<sub>4</sub>), **14** (C<sub>22</sub>H<sub>27</sub>NO<sub>4</sub>), and **15** (C<sub>22</sub>H<sub>25</sub>NO<sub>4</sub>) were established on the basis of HRESIMS and <sup>13</sup>C NMR data, respectively. The 1D NMR spectroscopic data of **13–15** (Tables 3 and 4) showed a close correlation with those of waltherione P (**16**).<sup>8</sup> Compared to waltherione P, the CH<sub>3</sub>-2 methyl group ( $\delta_{\text{H}}$  2.39, s, 3H;  $\delta_{\text{C}}$  13.4) in **16** was replaced by a hydroxymethyl ( $\delta_{\text{H}}$  4.74, s, 2H;  $\delta_{\text{C}}$  56.9, CH<sub>2</sub>OH-2) in **13**, the hydrogen H-19 ( $\delta_{\text{H}}$  7.12, t) in **16** was replaced by a hydroxy group at C-19 in **14**, and the CH<sub>2</sub>-15 methylene ( $\delta_{\text{H}}$  2.61, t;  $\delta_{\text{C}}$  36.6) was replaced by a carbonyl group ( $\delta_{\text{C}}$  203.0, C-15) in **15**. These assignments were respectively confirmed by the HMBC correlation signals from CH<sub>2</sub>OH-2 to C-2 ( $\delta_{\text{C}}$  147.2) and C-3 ( $\delta_{\text{C}}$  144.1) in **13**, from H-17/21 ( $\delta_{\text{H}}$  6.98, d) to C-19 ( $\delta_{\text{C}}$  156.4) in **14**, and from H-14 ( $\delta_{\text{H}}$  3.10, m) and H-17/21 ( $\delta_{\text{H}}$  7.40, d) to C-15 in **15**. To establish the absolute configuration at C-5, the ECD spectra of **13–15** were recorded and compared with previously published data.<sup>8,10</sup> The experimental spectra showed three positive CEs around 240, 280, and 310 nm and a negative CE at 355 nm (Figure 4), consistent with literature values for (*SS*)-stereoisomers.<sup>8,10</sup> Thus, the structures of compounds **13–15** (walindicaones H–J) were determined as shown.

The molecular formula of compound **17** (C<sub>19</sub>H<sub>29</sub>NO<sub>4</sub>) was established on the basis of HRESIMS and <sup>13</sup>C NMR data. The 1D NMR spectra of **17** showed a close resemblance to that of antidesmone (**18**).<sup>10</sup> The only difference observed was a hydroxymethyl ( $\delta_{\text{H}}$  4.74, s, 2H;  $\delta_{\text{C}}$  56.9, CH<sub>2</sub>OH-2) in **17** instead of the CH<sub>3</sub>-2 methyl group ( $\delta_{\text{H}}$  2.37, s, 3H;  $\delta_{\text{C}}$  14.5) in **18**. The HMBC correlations with C-2 ( $\delta_{\text{C}}$  147.2) and C-3 ( $\delta_{\text{C}}$  144.0) allowed positioning the methylene at C-2. The ECD spectrum of **17** was similar to those of **13–16** and **18**, with

Chart 2

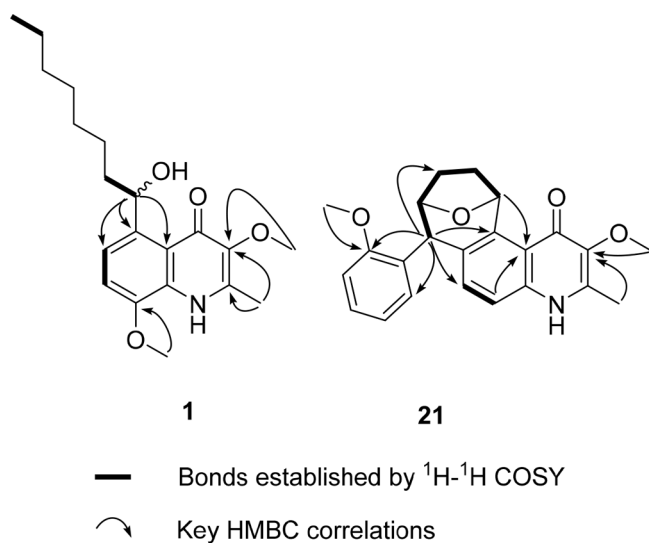
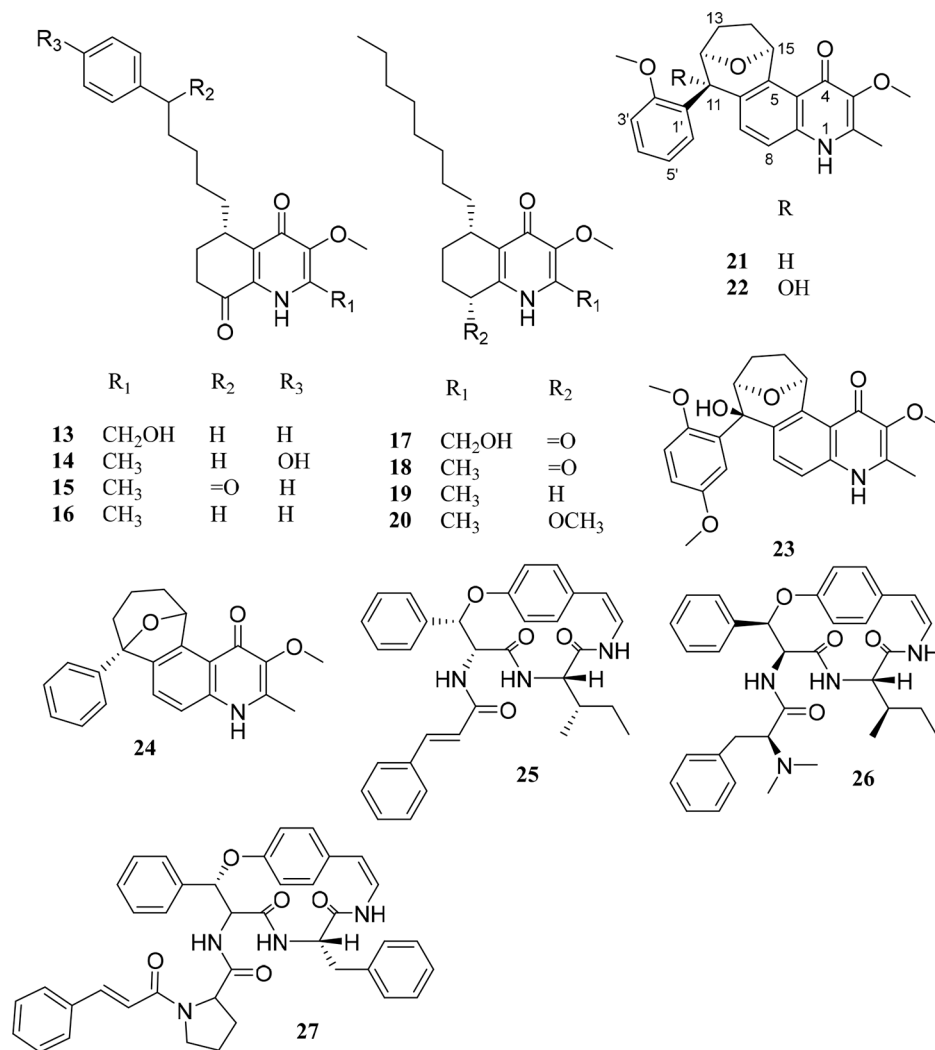


**Figure 1.** Key <sup>1</sup>H-<sup>1</sup>H COSY and HMBC correlations of compounds 1 and 21.

three positive CEs around 240, 280, and 310 nm and a negative CE at 355 nm (Figure 4).<sup>8,10</sup> Thus, the absolute configuration was established as 5*S*. The structure of 17

(walindicaone K) was identified as 2-(hydroxymethyl)-3-methoxy-5-octyl-1,5,6,7-tetrahydroquinoline-4,8-dione.

The molecular formula of compound 21 (C<sub>23</sub>H<sub>23</sub>NO<sub>4</sub>) was established on the basis of HRESIMS and <sup>13</sup>C NMR data. The <sup>1</sup>H and <sup>13</sup>C NMR spectra of 21 were closely related to those of waltherione A (22), indicating the presence of a 4-quinolone moiety fused to a bicyclic ether with an attached phenyl ring.<sup>12</sup> When compared with the molecular formula of waltherione A, that of 21 was one oxygen atom less. Analysis of the NMR data revealed that a hydroxy group in 22 was absent. Instead, an additional hydrogen atom ( $\delta_{\text{H}}$  5.29, d, H-11) was present in 21 and substituted at the same position (C-11). This observation was supported by the upfield shift of C-11 ( $\delta_{\text{C}}$  45.9 in 21 vs 77.2 in 22) and was confirmed by the HMBC correlation signals from H-11 to C-5 ( $\delta_{\text{C}}$  144.3), C-7 ( $\delta_{\text{C}}$  134.2), C-13 ( $\delta_{\text{C}}$  24.9), and C-2' ( $\delta_{\text{C}}$  160) (Figure 1). The NOESY correlation between H-12 and H-15 and the absence of a correlation between H-11 and H-15 indicated the *cis* configuration between H-12 and H-15 and the *trans* orientation between H-11 and H-15, respectively. This observation was confirmed by the (1*S*, 12*R*, 15*S*) absolute configurations determined by comparison of experimental and calculated ECD spectra (Figure 5) with a similarity score of 0.5954 and the enantiomer as 0.0154 with  $\sigma$  = 0.36 and a -6 nm shift as calculated by

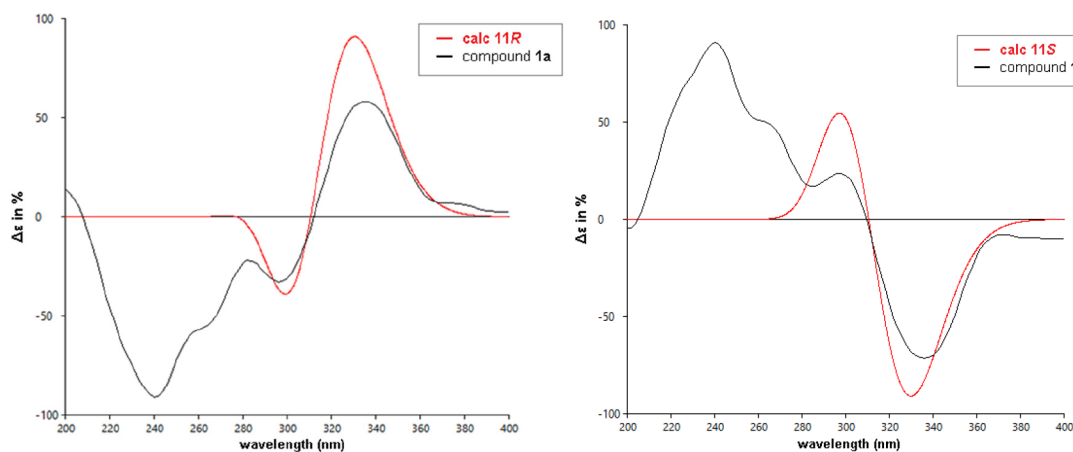


**Figure 2.** Experimental ECD spectra of **1a** and **1b** and comparison with the calculated spectrum for the (11*R*)-stereoisomer and (11*S*)-stereoisomer.

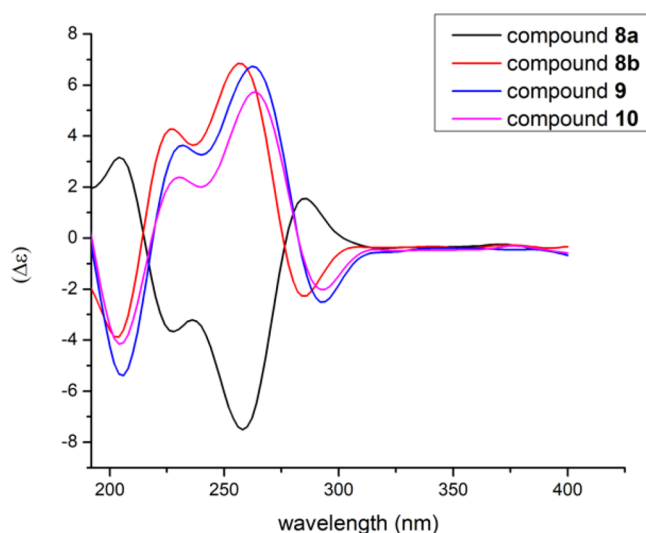


**Figure 3.** Experimental ECD spectra of **8a**, **8b**, **9**, and **10**.

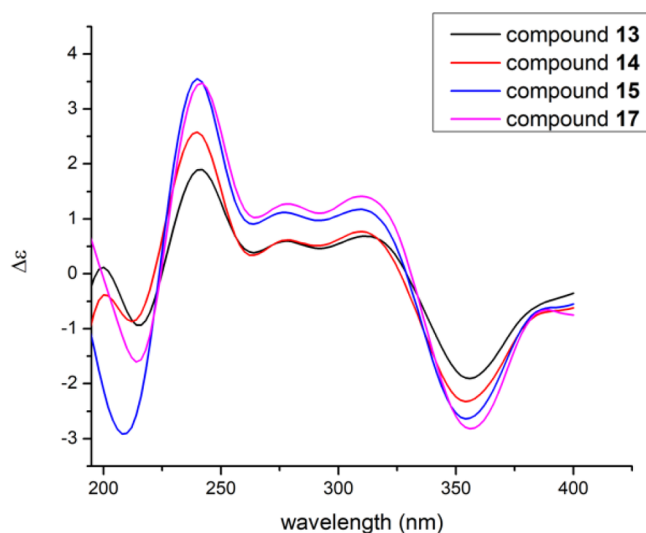


**Figure 4.** Experimental ECD spectra of **13–15** and **17**.

SpecDis.<sup>18</sup> Again, the distortions in the experimental spectrum are likely due to the dynamism of the hydroxypyridine–pyridone tautomerization that is not captured in the calculated

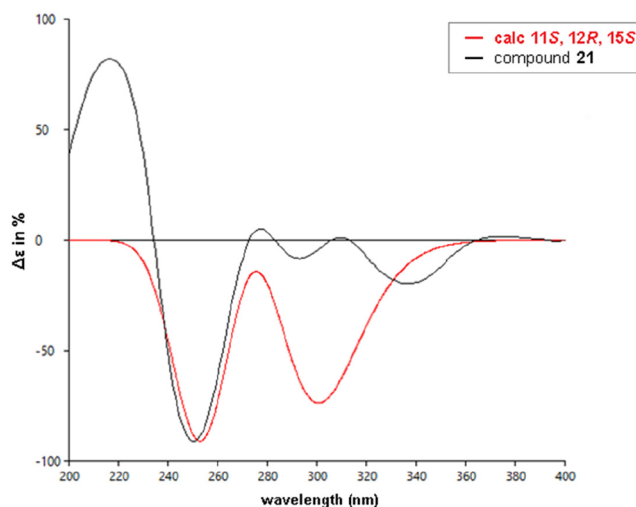


**Figure 5.** Experimental ECD spectra of **21** and comparison with the calculated spectrum for the (11*S*, 12*R*, 15*S*)-stereoisomer.

spectrum. Thus, compound **21** was identified as (11*S*,12*R*,15*S*)-11-dehydroxywaltherione A.

An early biological response of the immune system to infection, injury, or irritation results in inflammation.<sup>21</sup> Nuclear factor kappa-B (NF- $\kappa$ B), as a multidirectional, pleiotropic inflammation regulator, is at the core of inflammation-induced disorders.<sup>22</sup> Activation of NF- $\kappa$ B initiates the transcription of various inflammatory genes including cytokines, chemokines, and adhesion molecules, leading to the release of large quantities of inflammatory factors such as TNF- $\alpha$  and IL-1 $\beta$ , thereby enhancing and amplifying the inflammatory response.<sup>23,24</sup> In extreme cases, this may lead to a condition known as cytokine release syndrome or a cytokine storm, capable of causing organ damage. As summarized in Table 5, TNF- $\alpha$ -induced NF- $\kappa$ B activity with transfected human embryonic kidney cells 293 was inhibited by compounds **6**, **8a**, **9–11**, **13**, **21**, and **24** with IC<sub>50</sub> values of 10.2, 10.1, 10.3, 8.9, 12.1, 11.9, 7.2, and 7.1  $\mu$ M, respectively, which were comparable to the inhibitory activity of the positive control, BAY 11-7082 (IC<sub>50</sub> = 9.7  $\mu$ M). Under these experimental conditions, the compounds did not mediate a cytotoxic response at a concentration of 50  $\mu$ M.

**Table 5. Inhibition of NO Production in LPS-Stimulated RAW 264.7 Cells and TNF- $\alpha$ -Induced NF- $\kappa$ B Activity in Human Embryonic Kidney Cells 293 Determined with Compounds 1a–27**

compound	nitrite assay				NF- $\kappa$ B assay		
	% inhib. <sup>a</sup>	IC <sub>50</sub> ( $\mu$ M)	% surv. <sup>b</sup>	growth inhib. IC <sub>50</sub> ( $\mu$ M)	% inhib. <sup>c</sup>	IC <sub>50</sub> ( $\mu$ M)	% surv. <sup>d</sup>
1a	86.5 $\pm$ 0.7	25.8 $\pm$ 1.0	84.9 $\pm$ 9.2		<50		72.6 $\pm$ 7.2
1b	91.7 $\pm$ 2.1	25.8 $\pm$ 2.0	64.7 $\pm$ 6.2		<50		75.6 $\pm$ 6.5
2	<50		69.9 $\pm$ 7.2		<50		86.7 $\pm$ 3.3
3	63.8 $\pm$ 1.8	35.6 $\pm$ 2.2	86.5 $\pm$ 6.4		<50		75.8 $\pm$ 12.6
4	<50		70.2 $\pm$ 8.4		<50		83.6 $\pm$ 5.9
5	<50		59.3 $\pm$ 2.9		<50		83.5 $\pm$ 8.5
6	97.9 $\pm$ 0.7	11.4 $\pm$ 1.2	<50	33.3 $\pm$ 2.1	77.5 $\pm$ 4.8	10.2 $\pm$ 8.3	76.7 $\pm$ 19.7
7	<50		82.8 $\pm$ 5.8		<50		76.8 $\pm$ 15.8
8a	99.1 $\pm$ 0.2	12.8 $\pm$ 0.7	61.0 $\pm$ 7.0		81.6 $\pm$ 4.7	10.1 $\pm$ 5.8	91.8 $\pm$ 19.1
8b	97.2 $\pm$ 0.9	11.7 $\pm$ 0.8	84.3 $\pm$ 3.8		<50		77.2 $\pm$ 8.2
9	94.5 $\pm$ 2.5	18.8 $\pm$ 0.9	<50	25.9 $\pm$ 4.4	85.4 $\pm$ 2.2	10.3 $\pm$ 3.8	85.3 $\pm$ 6.0
10	<50		73.2 $\pm$ 7.5		97.9 $\pm$ 2.5	8.9 $\pm$ 1.8	82.7 $\pm$ 7.3
11	99.7 $\pm$ 0.3	11.0 $\pm$ 0.6	<50	32.2 $\pm$ 7.5	88.6 $\pm$ 6.0	12.1 $\pm$ 5.9	89.0 $\pm$ 4.6
12	<50		57.2 $\pm$ 7.6		<50		69.9 $\pm$ 2.2
13	79.1 $\pm$ 1.3	31.0 $\pm$ 1.2	50.8 $\pm$ 4.6		71.1 $\pm$ 2.5	11.9 $\pm$ 6.3	100 $\pm$ 13.9
14	<50		89.3 $\pm$ 4.7		<50		80.5 $\pm$ 9.7
15	<50		74.5 $\pm$ 4.3		<50		82.2 $\pm$ 6.8
16	59.7 $\pm$ 2.9	40.7 $\pm$ 3.1	67.5 $\pm$ 8.6		<50		88.4 $\pm$ 12.1
17	89.9 $\pm$ 1.8	25.4 $\pm$ 1.9	50.9 $\pm$ 7.1		<50		93.1 $\pm$ 13.9
18	97.4 $\pm$ 1.1	16.1 $\pm$ 0.6	63.5 $\pm$ 3.8		<50		85.8 $\pm$ 5.8
19	99.9 $\pm$ 0.2	20.8 $\pm$ 3.5	67.6 $\pm$ 1.9		<50		90.8 $\pm$ 10.1
20	60.3 $\pm$ 4.2	42.9 $\pm$ 2.8	51.4 $\pm$ 2.9		<50		90.3 $\pm$ 1.9
21	56.3 $\pm$ 3.4	38.8 $\pm$ 4.6	100 $\pm$ 2.0		84.5 $\pm$ 2.5	7.2 $\pm$ 2.8	79.6 $\pm$ 9.8
22	<50		100 $\pm$ 9.2		<50		86.7 $\pm$ 2.6
23	<50		100 $\pm$ 9.9		<50		74.5 $\pm$ 12.2
24	58.7 $\pm$ 2.2	35.7 $\pm$ 3.3	100 $\pm$ 4.2		78.0 $\pm$ 1.7	7.1 $\pm$ 4.3	89.0 $\pm$ 24.3
25	58.5 $\pm$ 3.7	43.0 $\pm$ 3.6	100 $\pm$ 9.1		<50		100 $\pm$ 6.7
26	<50		94.8 $\pm$ 11		<50		86.4 $\pm$ 24.3
27	63.7 $\pm$ 2.1	32.0 $\pm$ 1.8	100 $\pm$ 0.5		<50		76.6 $\pm$ 8.5
L-NMMA <sup>e</sup>		22.7 $\pm$ 1.8					
BAY 11-7082 <sup>f</sup>						9.7 $\pm$ 3.9	

<sup>a</sup>% inhibition at a concentration of 50  $\mu$ M. <sup>b</sup>% survival at a concentration of 50  $\mu$ M. <sup>c</sup>% inhibition of NF- $\kappa$ B at 50  $\mu$ M. <sup>d</sup>% survival at concentration of 50  $\mu$ M. <sup>e</sup>Positive control for NO. <sup>f</sup>Positive control for NF- $\kappa$ B.

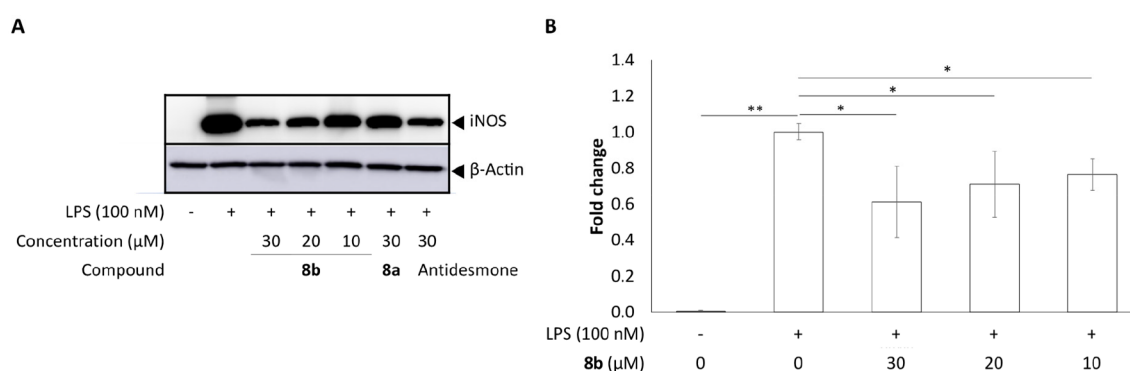


**Figure 6.** (A) Effect of compounds 8a/8b on the expression of iNOS protein in LPS-stimulated RAW 264.7 cells. (B) RAW 264.7 cells were pretreated with 8b (10, 20, 30  $\mu$ M) for 15 min and then stimulated with LPS (100 ng/mL) for 4 h. Controls included no treatment or treatment with LPS alone. The relative expression levels of iNOS mRNA (*Nos2*) were determined by qPCR. *Gapdh* was used for the normalization of *Nos2*. The data represent the means  $\pm$  standard deviation of three independent experiments (\* $p$  < 0.05, \*\* $p$  < 0.001).

It is known that inhibition of aberrantly active NF- $\kappa$ B activity correlates with the inhibition of NO production.<sup>25</sup> Nitric oxide (NO) is one of the major inflammatory mediators. Excessive production has detrimental effects on multiple organs of the body, leading to tissue damage.<sup>26</sup> Natural products that reduce NO production by down-regulation of

inducible nitric oxide synthase (iNOS), without affecting endothelial NOS (eNOS) or neuronal NOS (nNOS), may be of value for development as anti-inflammatory agents.<sup>27</sup> Accordingly, all isolates were evaluated for the potential of inhibiting lipopolysaccharide (LPS)-induced NO production with murine macrophage RAW 264.7 cells.

Compounds **6**, **8a**, **8b**, and **11** demonstrated the most potent NO inhibitory activities (Table 5). IC<sub>50</sub> values ranged from 11.0 to 12.8 μM, indicating greater activity than a positive control, L-N<sup>G</sup>-monomethyl arginine citrate (L-NMMA), with an IC<sub>50</sub> value of 22.7 μM (Table 5). However, **6** and **11** lacked specificities in that they mediated cytotoxic responses with IC<sub>50</sub> values of 33.3 and 32.2 μM, respectively. Compounds **1a**, **1b**, **9**, and **17–19** showed NO inhibitory activity comparable to the positive control, with IC<sub>50</sub> values ranging from 16.1 to 25.8 μM. Among these compounds, compound **9** induced a cytotoxic response with an IC<sub>50</sub> of 25.9 μM. Compounds **3**, **13**, **16**, **20**, **21**, **24**, **25**, and **27** exhibited moderate NO inhibitory activity, with IC<sub>50</sub> values ranging from 31.0 to 43.0 μM, without cytotoxicity.

These results indicate that NO inhibitory activity is affected by the C-8 substituent; carbonylation, hydroxylation, or hydroxymethylation significantly decreased activity. In addition, *p*-hydroxy substitution on the terminal benzene ring and carbonylation at C-15 reduced the inhibitory response.

The pro-inflammatory enzyme iNOS plays a critical role in inflammatory events by regulating NO production.<sup>28</sup> As described above, of the compounds tested, **6**, **8a**, **8b**, and **11** reduced NO activity to the greatest extent. Since **6** and **11** demonstrated concomitant cell growth inhibition, **8a** and **8b** were considered the most promising compounds. As illustrated in Figure 6, some preliminary follow-up studies were performed. As expected, treatment of cultured RAW 264.7 cells with 100 nM LPS markedly stimulated the expression of iNOS at both the protein (Figure 6A) and mRNA levels (Figure 6B). We did not measure the protein expression levels of eNOS and nNOS because the protein expression levels of eNOS and nNOS are negligible in RAW 264.7 cells.<sup>29</sup> At a concentration of 30 μM, **8b** inhibited the level of iNOS protein with potency similar to an equimolar concentration of the positive control, antidesmone. Surprisingly, **8a** was less active than **8b**; at a concentration of 30 μM, the response mediated by **8a** was similar to the response mediated by **8b** at a concentration of 10 μM. At the level of transcription, the reduction of iNOS mRNA expression mediated by **8b** correlated with the reduction of protein levels, indicating a causative effect.

However, the mode of transcriptional regulation yet remains to be determined. As shown in Table 5, **8b** was not an effective inhibitor of TNF-α-induced NF-κB activity with transfected human embryonic kidney cells 293. On the other hand, **8a** was an effective inhibitor of TNF-α-induced NF-κB activity, but failed to reduce the expression of iNOS (Figure 6A), even though the generation of NO was reduced (IC<sub>50</sub> = 12.8 μM) with efficacy similar to **8b** (IC<sub>50</sub> = 11.7 μM). It would be of interest to define the molecular details of this conundrum in future studies. As it stands, it appears the structural configuration of **8** does have a bearing on activity, and it seems possible that the response induced by combining the enantiomers could be superior to either one individually.

In any case, given the potential of various chemical constituents derived from *W. indica* to reduce NO generation, inhibit the expression of iNOS, and diminish the activity of NF-κB, evidence is provided herein to support the traditional use of this plant material for the treatment of inflammatory-associated disorders.

## EXPERIMENTAL SECTION

**General Experimental Procedures.** Optical rotations were recorded in MeOH on a Rudolph Research AUTOPOL IV multiwavelength polarimeter (Rudolph Research Analytical, Hackettstown, NJ, USA). Ultraviolet spectra were measured with a Shimadzu PharmaSpec-1800 UV-visible spectrophotometer (Shimadzu Scientific Instruments, MD, USA). Electronic circular dichroism spectra were obtained at 20 °C on a JASCO J-815 spectropolarimeter (JASCO Inc., Tokyo, Japan). Infrared radiation spectra were recorded on a Thermo Scientific Nicolet iS 10 FT-IR spectrometer (Thermo Fisher Scientific, Waltham, MA, USA). 1D- and 2D-NMR spectra were collected on a Bruker AVANCE DRX-400 NMR spectrometer (Bruker, Billerica, MA, USA), and the data were processed using TopSpin 3.2 software. High-resolution electrospray ionization mass spectra were performed with an Agilent 6530 LC-qTOF High Mass Accuracy mass spectrometer (Santa Clara, CA, USA) under the positive-ion mode. Silica gel (230–400 mesh, 480–800 mesh, Sorbent Technologies, Atlanta, GA, USA), Sephadex LH-20 (GE Healthcare, Piscataway, NJ, USA), and MCI gel (CHP-20P, Mitsubishi Chemical Corporation, Tokyo, Japan) were used for column chromatography. Preparative HPLC was performed on a Thermo Scientific Ultimate 3000 system equipped with a photodiode array detector using a YMC reversed-phase C<sub>18</sub> column (5 μm, 20 × 250 mm, YMC-pack ODS-A) with a flow rate of 5 mL/min or a reversed-phase C<sub>18</sub> chiral column (250 × 10 mm, 5 μm, Cellulose-1) with a flow rate of 4 mL/min.

**Plant Material.** Fresh roots of *W. indica* were collected from Puako, Hawai'i Island (Big Island), Hawaii, United States, in November 2019 and were identified by Kumu Dane Kaohelani Silva. A voucher specimen (No. WIS01) was deposited at the Natural Product Chemistry Laboratory, Daniel K. Inouye College of Pharmacy, University of Hawaii at Hilo.

**Extraction and Isolation.** The powdered roots (11.5 kg) of *W. indica* were extracted with MeOH (60 L), three times, at room temperature. The extract was filtered and concentrated under reduced pressure, to afford a crude extract (1620 g), and then successively extracted with *n*-hexane and EtOAc. After solvent removal, the EtOAc-soluble partition (105.0 g) was separated on a MCI gel CHP-20P column, eluted with H<sub>2</sub>O–MeOH (1:0 to 0:1, v/v) and finally with acetone, to yield seven fractions. The 80% MeOH fraction (13.0 g) was chromatographed over a silica gel column (*n*-hexane–EtOAc, 100:0 to 0:100, and finally CHCl<sub>3</sub>–MeOH, 1:1) to yield 18 fractions (Fr. 1–18), which were combined on the basis of thin-layer chromatography analysis. Fr. 4 (520.0 mg) was applied to a Sephadex LH-20 column eluting with MeOH to afford three fractions (4.1–4.3). Fr. 4.3 (310.0 mg) was separated on a silica gel column (CHCl<sub>3</sub>–MeOH, 200:1 to 50:1) to yield compound **18** (195.0 mg) and one subfraction, 4.3.1. Subfraction 4.3.1 (63.0 mg) was further purified on a silica gel column (*n*-hexane–*i*-PrOH, 7:1) to yield compounds **3** (3.6 mg) and **4** (17.6 mg). Fr. 5 (650.0 mg) was loaded on a Sephadex LH-20 column with MeOH as eluent to give two fractions (5.1 and 5.2). Fr. 5.1 (500.0 mg) was chromatographed on a silica gel column (*n*-hexane–*i*-PrOH, 20:1, 8:1, and 3:1) to yield compound **16** (33.2 mg). Fr. 5.2 (80.0 mg) was separated on a silica gel column (*n*-hexane–acetone, 4:1, 3:1, and 2:1) and further purified by preparative HPLC (MeOH–H<sub>2</sub>O, 60:40 to 95:5) to furnish compound **5** (3.0 mg). Fr. 6 (1.84 g) was separated on a silica gel column (CHCl<sub>3</sub>–acetone, 20:1 to 1:1) to obtain 13 fractions (6.1–6.13). Fr. 6.4 (118.0 mg) was separated on a silica gel column (*n*-hexane–acetone, 4:1 and 2:1) to furnish compound **25** (62.6 mg). Fr. 6.6 (110.0 mg) was separated on a silica gel column (CHCl<sub>3</sub>–MeOH, 500:1, 300:1, and 200:1) and purified by preparative HPLC (MeCN–H<sub>2</sub>O, 45:55 to 60:40) to furnish compounds **15** (5.9 mg), **7** (3.6 mg), **2** (7.5 mg), and **1**. Compound **1** (9.3 mg) was further purified by preparative chiral-phase HPLC (MeCN–H<sub>2</sub>O, 55:45) to furnish compounds **1a** (3.0 mg) and **1b** (3.3 mg). Fr. 6.7 (405.0 mg) was chromatographed on a silica gel column (*n*-hexane–acetone, 4:1 to 1:1) to yield **26** (57.7 mg), **24** (70.5 mg), and seven subfractions (6.7.1–6.7.7). Subfraction 6.7.4 (22.5 mg) was subjected to a silica

gel column (CHCl<sub>3</sub>–MeOH, 400:1, 300:1, and 200:1) to yield compounds **17** (9.8 mg) and **13** (5.5 mg). Subfraction 6.7.7 (42.5 mg) was further purified by preparative HPLC (MeCN–H<sub>2</sub>O, 40:60) to furnish compound **21** (25.7 mg). Fr. 6.9 (146.0 mg) was separated on a silica gel column (CHCl<sub>3</sub>–MeOH, 200:1, 100:1, and 50:1) and further purified on another silica gel column (*n*-hexane–*i*-PrOH, 4:1) to yield compounds **14** (5.0 mg), **22** (77.0 mg), and **23** (23.2 mg). Fr. 8 (1.60 g) was subjected to a silica gel column (CHCl<sub>3</sub>–MeOH, 1000:1, 800:1, 400:1, 300:1, 200:1, 100:1, 50:1, and 20:1) to yield compounds **20** (77.3 mg) and **11** (123.6 mg) and six fractions (8.1–8.6). Fr. 8.5 (56.7 mg) was further purified by preparative HPLC (MeCN–H<sub>2</sub>O, 45:55) to furnish compounds **9** (17.8 mg) and **19** (8.4 mg). The 100% MeOH fraction (12.0 g) was chromatographed over a silica gel column (CHCl<sub>3</sub>–MeOH, 100:1 to 2:1) to yield 12 fractions (Fr. 19–30). Fr. 23 (565.0 mg) was chromatographed on a silica gel column (CHCl<sub>3</sub>–MeOH, 1000:1 to 30:1) to yield seven fractions (23.1–23.7). Fr. 23.1 (100.5 mg) was subjected to a silica gel column (*n*-hexane–acetone, 10:1 to 4:1) and further purified by preparative HPLC (MeOH–H<sub>2</sub>O, 60:40 to 95:5) to furnish compounds **27** (28.4 mg) and **6** (4.0 mg). Fr. 28 (520 mg) was subjected to a silica gel column (CHCl<sub>3</sub>–MeOH, 500:1, 400:1, 300:1, 200:1, 100:1, 50:1, 20:1, and 10:1) to yield compound **8** and four fractions (28.1–28.4). Compound **8** (33.3 mg) was further purified by preparative chiral-phase HPLC (MeCN–H<sub>2</sub>O, 55:45) to furnish compounds **8a** (12.5 mg) and **8b** (15.5 mg). Fr. 28.1 (58.0 mg) was further purified by preparative HPLC (MeOH–H<sub>2</sub>O, 75:25) to furnish compounds **10** (7.9 mg) and **12** (29.6 mg).

**Compound 1a:** pale-yellow oil;  $[\alpha]_{\text{D}}^{20}$  11 (*c* 0.1, MeOH); UV<sub>max</sub> (MeOH)  $\lambda_{\text{max}}$  (log  $\epsilon$ ) 331 (3.89), 240 (4.40) nm; IR (film)  $\nu_{\text{max}}$  3300, 2925, 2854, 1626, 1571, 1524, 1422, 1261, 1233, 1021 cm<sup>-1</sup>; CD (MeOH)  $\lambda_{\text{max}}$  ( $\Delta\epsilon$ ) 240 (–2.69), 336 (+1.72) nm; <sup>1</sup>H NMR data, see Table 1; <sup>13</sup>C NMR data, see Table 2; HRESIMS *m/z* 348.2172 [M + H]<sup>+</sup> (calcd for C<sub>20</sub>H<sub>30</sub>NO<sub>4</sub>, 348.2175).

**Compound 1b:** pale-yellow oil;  $[\alpha]_{\text{D}}^{20}$  –11 (*c* 0.15, MeOH); UV<sub>max</sub> (MeOH)  $\lambda_{\text{max}}$  (log  $\epsilon$ ) 331 (3.94), 240 (4.47) nm; IR (film)  $\nu_{\text{max}}$  2923, 2854, 1626, 1568, 1520, 1421, 1260, 1232, 1087 cm<sup>-1</sup>; CD (MeOH)  $\lambda_{\text{max}}$  ( $\Delta\epsilon$ ) 240 (+3.07), 336 (–2.41) nm; <sup>1</sup>H NMR data, see Table 1; <sup>13</sup>C NMR data, see Table 2; HRESIMS *m/z* 348.2173 [M + H]<sup>+</sup> (calcd for C<sub>20</sub>H<sub>30</sub>NO<sub>4</sub>, 348.2175).

**Compound 2:** pale-yellow oil;  $[\alpha]_{\text{D}}^{20}$  0 (*c* 0.1, MeOH); UV<sub>max</sub> (MeOH)  $\lambda_{\text{max}}$  (log  $\epsilon$ ) 328 (4.00), 233 (4.28) nm; IR (film)  $\nu_{\text{max}}$  2926, 2854, 1688, 1622, 1570, 1523, 1244, 1089, 1020 cm<sup>-1</sup>; <sup>1</sup>H NMR data, see Table 1; <sup>13</sup>C NMR data, see Table 2; HRESIMS *m/z* 346.2016 [M + H]<sup>+</sup> (calcd for C<sub>20</sub>H<sub>28</sub>NO<sub>4</sub>, 346.2018).

**Compound 3:** colorless oil;  $[\alpha]_{\text{D}}^{20}$  0 (*c* 0.25, MeOH); UV<sub>max</sub> (MeOH)  $\lambda_{\text{max}}$  (log  $\epsilon$ ) 331 (3.56), 235 (4.08) nm; IR (film)  $\nu_{\text{max}}$  3270, 2929, 2853, 1704, 1625, 1575, 1527, 1258, 1237, 1085, 1018 cm<sup>-1</sup>; <sup>1</sup>H NMR data, see Table 1; <sup>13</sup>C NMR data, see Table 2; HRESIMS *m/z* 346.2017 [M + H]<sup>+</sup> (calcd for C<sub>20</sub>H<sub>28</sub>NO<sub>4</sub>, 346.2018).

**Compound 4:** colorless oil;  $[\alpha]_{\text{D}}^{20}$  0 (*c* 0.12, MeOH); UV<sub>max</sub> (MeOH)  $\lambda_{\text{max}}$  (log  $\epsilon$ ) 335 (3.80), 239 (4.33) nm; IR (film)  $\nu_{\text{max}}$  2924, 2852, 1622, 1586, 1564, 1499, 1468, 1423, 1386, 1281, 1229, 1053 cm<sup>-1</sup>; <sup>1</sup>H NMR data, see Table 1; <sup>13</sup>C NMR data, see Table 2; HRESIMS *m/z* 318.2066 [M + H]<sup>+</sup> (calcd for C<sub>19</sub>H<sub>28</sub>NO<sub>3</sub>, 318.2069).

**Compound 5:** pale-yellow oil;  $[\alpha]_{\text{D}}^{20}$  0 (*c* 0.48, MeOH); UV<sub>max</sub> (MeOH)  $\lambda_{\text{max}}$  (log  $\epsilon$ ) 335 (3.92), 239 (4.44) nm; IR (film)  $\nu_{\text{max}}$  2925, 2852, 1584, 1564, 1463, 1418, 1253, 1047 cm<sup>-1</sup>; <sup>1</sup>H NMR data, see Table 1; <sup>13</sup>C NMR data, see Table 2; HRESIMS *m/z* 352.1908 [M + H]<sup>+</sup> (calcd for C<sub>22</sub>H<sub>26</sub>NO<sub>3</sub>, 352.1913).

**Compound 6:** pale-yellow oil;  $[\alpha]_{\text{D}}^{20}$  0 (*c* 0.13, MeOH); UV<sub>max</sub> (MeOH)  $\lambda_{\text{max}}$  (log  $\epsilon$ ) 327 (3.90), 240 (4.32) nm; IR (film)  $\nu_{\text{max}}$  2925, 2853, 1633, 1561, 1505, 1465, 1266, 1017 cm<sup>-1</sup>; <sup>1</sup>H NMR data, see Table 1; <sup>13</sup>C NMR data, see Table 2; HRESIMS *m/z* 336.1961 [M + H]<sup>+</sup> (calcd for C<sub>22</sub>H<sub>26</sub>NO<sub>2</sub>, 336.1964).

**Compound 7:** pale-yellow oil;  $[\alpha]_{\text{D}}^{20}$  0 (*c* 0.12, MeOH); UV<sub>max</sub> (MeOH)  $\lambda_{\text{max}}$  (log  $\epsilon$ ) 328 (3.84), 233 (4.22) nm; IR (film)  $\nu_{\text{max}}$  2927, 2855, 1687, 1621, 1570, 1523, 1245, 1089, 1019 cm<sup>-1</sup>; <sup>1</sup>H NMR data,

see Table 1; <sup>13</sup>C NMR data, see Table 2; HRESIMS *m/z* 380.1860 [M + H]<sup>+</sup> (calcd for C<sub>23</sub>H<sub>26</sub>NO<sub>4</sub>, 380.1862).

**Compound 8a:** colorless oil;  $[\alpha]_{\text{D}}^{20}$  –81 (*c* 0.19, MeOH); UV<sub>max</sub> (MeOH)  $\lambda_{\text{max}}$  (log  $\epsilon$ ) 270 (3.94), 204 (4.27) nm; IR (film)  $\nu_{\text{max}}$  2927, 2854, 1618, 1496, 1432, 1270, 1014 cm<sup>-1</sup>; CD (MeOH)  $\lambda_{\text{max}}$  ( $\Delta\epsilon$ ) 204 (+3.17), 228 (–3.67), 258 (–7.51), 286 (+1.55) nm; <sup>1</sup>H NMR data, see Table 1; <sup>13</sup>C NMR data, see Table 2; HRESIMS *m/z* 340.2276 [M + H]<sup>+</sup> (calcd for C<sub>22</sub>H<sub>30</sub>NO<sub>2</sub>, 340.2277).

**Compound 9:** pale-yellow oil;  $[\alpha]_{\text{D}}^{20}$  75 (*c* 0.41, MeOH); UV<sub>max</sub> (MeOH)  $\lambda_{\text{max}}$  (log  $\epsilon$ ) 278 (4.10), 222 (4.35), 201 (4.35) nm; IR (film)  $\nu_{\text{max}}$  2928, 2854, 1603, 1597, 1512, 1452, 1276, 1247, 1068, 1011 cm<sup>-1</sup>; CD (MeOH)  $\lambda_{\text{max}}$  ( $\Delta\epsilon$ ) 206 (–5.39), 232 (+3.62), 262 (+6.73), 292 (–2.50) nm; <sup>1</sup>H NMR data, see Table 3; <sup>13</sup>C NMR data, see Table 4; HRESIMS *m/z* 386.2328 [M + H]<sup>+</sup> (calcd for C<sub>23</sub>H<sub>32</sub>NO<sub>4</sub>, 386.2331).

**Compound 10:** colorless oil;  $[\alpha]_{\text{D}}^{20}$  54 (*c* 0.26, MeOH); UV<sub>max</sub> (MeOH)  $\lambda_{\text{max}}$  (log  $\epsilon$ ) 279 (4.00), 226 (4.21), 202 (4.37) nm; IR (film)  $\nu_{\text{max}}$  3407, 2935, 2858, 1679, 1548, 1447, 1277, 1129, 1067, 1009 cm<sup>-1</sup>; CD (MeOH)  $\lambda_{\text{max}}$  ( $\Delta\epsilon$ ) 204 (–4.15), 230 (+2.39), 264 (+5.73), 292 (–2.02) nm; <sup>1</sup>H NMR data, see Table 3; <sup>13</sup>C NMR data, see Table 4; HRESIMS *m/z* 384.2176 [M + H]<sup>+</sup> (calcd for C<sub>23</sub>H<sub>30</sub>NO<sub>4</sub>, 384.2175).

**Compound 13:** pale-yellow oil;  $[\alpha]_{\text{D}}^{20}$  22 (*c* 0.18, MeOH); UV<sub>max</sub> (MeOH)  $\lambda_{\text{max}}$  (log  $\epsilon$ ) 331 (3.30), 245 (3.98), 203 (4.03) nm; IR (film)  $\nu_{\text{max}}$  3331, 2926, 2855, 1694, 1613, 1556, 1453, 1391, 1252, 1033 cm<sup>-1</sup>; CD (MeOH)  $\lambda_{\text{max}}$  ( $\Delta\epsilon$ ) 216 (–0.94), 242 (+1.90), 278 (+0.60), 312 (+0.68), 356 (–1.91) nm; <sup>1</sup>H NMR data, see Table 3; <sup>13</sup>C NMR data, see Table 4; HRESIMS *m/z* 370.2018 [M + H]<sup>+</sup> (calcd for C<sub>22</sub>H<sub>28</sub>NO<sub>4</sub>, 370.2018).

**Compound 14:** colorless oil;  $[\alpha]_{\text{D}}^{20}$  26 (*c* 0.17, MeOH); UV<sub>max</sub> (MeOH)  $\lambda_{\text{max}}$  (log  $\epsilon$ ) 331 (3.36), 276 (3.37), 244 (4.05) nm; IR (film)  $\nu_{\text{max}}$  3223, 2925, 2854, 1693, 1611, 1552, 1513, 1452, 1397, 1270, 1230, 1033, 1019 cm<sup>-1</sup>; CD (MeOH)  $\lambda_{\text{max}}$  ( $\Delta\epsilon$ ) 212 (–0.87), 240 (+2.58), 278 (+0.61), 310 (+0.77), 354 (–2.32) nm; <sup>1</sup>H NMR data, see Table 3; <sup>13</sup>C NMR data, see Table 4; HRESIMS *m/z* 370.2016 [M + H]<sup>+</sup> (calcd for C<sub>22</sub>H<sub>28</sub>NO<sub>4</sub>, 370.2018).

**Compound 15:** pale-yellow oil;  $[\alpha]_{\text{D}}^{20}$  36 (*c* 0.20, MeOH); UV<sub>max</sub> (MeOH)  $\lambda_{\text{max}}$  (log  $\epsilon$ ) 326 (3.43), 241 (4.31), 204 (4.70) nm; IR (film)  $\nu_{\text{max}}$  3224, 2929, 2854, 1682, 1612, 1553, 1513, 1449, 1397, 1272, 1204, 1033 cm<sup>-1</sup>; CD (MeOH)  $\lambda_{\text{max}}$  ( $\Delta\epsilon$ ) 208 (–2.91), 240 (+3.55), 278 (+1.12), 310 (+1.17), 354 (–2.64) nm; <sup>1</sup>H NMR data, see Table 3; <sup>13</sup>C NMR data, see Table 4; HRESIMS *m/z* 368.1859 [M + H]<sup>+</sup> (calcd for C<sub>22</sub>H<sub>26</sub>NO<sub>4</sub>, 368.1862).

**Compound 17:** colorless oil;  $[\alpha]_{\text{D}}^{20}$  42 (*c* 0.32, MeOH); UV<sub>max</sub> (MeOH)  $\lambda_{\text{max}}$  (log  $\epsilon$ ) 331 (3.45), 246 (4.15), 201 (4.12) nm; IR (film)  $\nu_{\text{max}}$  3330, 2923, 2854, 1694, 1612, 1557, 1514, 1391, 1251, 1177, 1033 cm<sup>-1</sup>; CD (MeOH)  $\lambda_{\text{max}}$  ( $\Delta\epsilon$ ) 214 (–1.60), 242 (+3.47), 278 (+1.27), 310 (+1.41), 356 (–2.82) nm; <sup>1</sup>H NMR data, see Table 3; <sup>13</sup>C NMR data, see Table 4; HRESIMS *m/z* 336.2177 [M + H]<sup>+</sup> (calcd for C<sub>19</sub>H<sub>30</sub>NO<sub>4</sub>, 336.2175).

**Compound 21:** pale-yellow oil;  $[\alpha]_{\text{D}}^{20}$  –20 (*c* 0.62, MeOH); UV<sub>max</sub> (MeOH)  $\lambda_{\text{max}}$  (log  $\epsilon$ ) 331 (3.66), 247 (4.26), 217 (4.26), 200 (4.35) nm; IR (film)  $\nu_{\text{max}}$  2934, 1632, 1555, 1512, 1491, 1286, 1243, 1107 cm<sup>-1</sup>; CD (MeOH)  $\lambda_{\text{max}}$  ( $\Delta\epsilon$ ) 216 (+2.68), 250 (–1.00), 340 (–0.62) nm; <sup>1</sup>H NMR data, see Table 3; <sup>13</sup>C NMR data, see Table 4; HRESIMS *m/z* 378.1706 [M + H]<sup>+</sup> (calcd for C<sub>23</sub>H<sub>24</sub>NO<sub>4</sub>, 378.1705).

**Cell Culture.** RAW 264.7 murine macrophage (TIB-71, ATCC) and human embryonic kidney 293/NF- $\kappa$ B-Luc cell lines (Panomics, Fremont, CA, USA) were maintained in Dulbecco's modified Eagle medium (DMEM) supplemented with heat-inactivated fetal bovine serum (FBS, 10%) and antibiotics (penicillin 100 IU/mL and streptomycin 100  $\mu$ g/mL) at 37 °C in a humidified incubator with 5% CO<sub>2</sub> in air.

**Inhibition of Nitric Oxide Production in Lipopolysaccharide-Activated Murine Macrophage RAW 264.7 Cells.** RAW 264.7 cells were plated at a density of 1  $\times$  10<sup>5</sup> cells per well in 96-well tissue culture-treated plates and incubated for 24 h. The media was removed, and the cells were pretreated with phenol red-free DMEM containing various concentrations of test compounds for 15 min and

then induced with 100 ng/mL of LPS from *Escherichia coli* O111:B4 (L2630, Sigma-Aldrich, Burlington, MA, USA) for an additional 20 h. Culture media (100  $\mu$ L) from each well was transferred to a clear-bottom 96-well plate, and Griess reagent was added to estimate the amount of nitrite. To evaluate the growth inhibitory effects of samples on RAW 264.7 cells under the same experimental conditions, cells were further incubated with Cell Counting Kit-8 (CCK-8, Dojindo Molecular Technologies Inc., Rockville, MD, USA) for an hour.<sup>30</sup> The IC<sub>50</sub> values were calculated using TableCurve software 2D (version 4) curve-fitting software (Jandel Scientific).

**iNOS mRNA Expression.** The purity and the quantity of total RNA extracted from RAW 264.7 cells were measured using a Biospecnano spectrophotometer (Shimadzu). gDNA was degraded by a master mix of iScript DNase and iScript DNase buffer (Bio-Rad). Then, iScript reverse transcription supermix was added to DNase-treated RNA samples and incubated at 25 °C for 5 min, 46 °C for 20 min, and 95 °C for 1 min. The resultant cDNA was used for quantitative real-time PCR (qPCR) to measure the gene expression levels of *Nos2* and a housekeeping gene, *Gapdh*. SYBR Green dye-based detection was implemented for qPCR with iTaq Universal SYBR Green super mix (Biorad, catalogue number 1725121) and primer pairs for *Nos2* (forward: 5'-GGA GCG AGT TGT GGA TTG TC-3', reverse: 5'-GTG AGG GCT TGG CTG AGT GAG-3') and *Gapdh* (forward: 5'-AAC GAC CCC TTC ATT GAC-3', reverse: 5'-TCC ACG ACA TAC TCA GCA C-3'). The fluorescence signal from SYBR Green was detected using a LightCycler 480 Instrument II, and the crossing point (Cp) value of each sample was obtained with LightCycler 480 analysis software. The LightCycler was purchased from Roche Life Science. The relative fold gene expression was calculated using the  $2^{-\Delta\Delta C_T}$  method.<sup>31</sup>

**Western Blot Analysis.** RAW 264.7 cells were plated at a density of  $5 \times 10^5$  cells per well in a 24-well tissue culture-treated plate. Cells were harvested and lysed using 1 $\times$  cell lysis buffer (Cell Signaling Technology) according to the manufacturer's instructions. After 5 min of incubation with lysis buffer, cells were centrifuged at 14000g for 10 min at 4 °C, and the supernatant as cell lysate was collected and stored at -80 °C until use. After quantification of protein using the BCA assay, equal amounts of total protein (20  $\mu$ g) in each cell lysate were resolved using SDS-PAGE (10%), and electrotransferred to PVDF membranes. The membranes were incubated with 5% skimmed milk in 0.1% Tween 20 containing TBS for 1 h at room temperature to block nonspecific protein binding. Then, membranes were incubated overnight at 4 °C with corresponding primary antibodies in 3% skimmed milk in TBS (1:1000 dilution for iNOS, 1:3000 dilution for  $\beta$ -actin) followed by incubation with horseradish peroxidase-conjugated secondary antibodies and visualization using an ECL detection kit with an Amersham Imager 600 (General Electronics).

**Inhibition of Tumor Necrosis Factor-alpha (TNF- $\alpha$ )-Induced NF- $\kappa$ B Activity.** 293/NF- $\kappa$ B-Luc cells (Panomic, Fremont, CA, USA) were plated at  $2 \times 10^4$  cells per well in white 96-well plates for measuring the transcriptional activity of NF- $\kappa$ B and clear 96-well plates for measuring cell viability. After 48 h of incubation, the culture media were discarded and fresh media containing either vehicle control (0.5% DMSO, v/v) or test samples were added to the cells in both white and clear plates. After 15 min of preincubation, TNF- $\alpha$  (ProSci Inc., Flint Place Poway, CA, USA) was added at a concentration of 2.5 ng/mL for 6 h. The cultured medium was removed from the white plates and the cells were rinsed once with PBS. Cells were incubated with 50  $\mu$ L of 1 $\times$  passive lysis buffer (Promega, Madison, WI, USA) on a shaker at room temperature for 15 min. The luminescence from each well was measured after adding luciferase assay substrate in Luciferase Assay Buffer II (Promega). Clear plates, which were treated in the same manner, were used to evaluate the growth inhibitory effects of test samples. MTT (0.5 mg/mL) was added and incubated for 2 h. The absorbance was measured at 570 nm.<sup>32</sup> The IC<sub>50</sub> values were calculated using TableCurve software 2D (version 4) curve-fitting software (Jandel Scientific).

**Computational Methods.** For ECD prediction, conformers within 5 kcal/mol of the lowest energy conformer were searched

using the Monte Carlo multiple minimum (MCMM) method<sup>33</sup> and the OPLS-2005 force field<sup>34</sup> in Schrodinger Inc.'s MacroModel<sup>35</sup> and then optimized in Gaussian 09<sup>36</sup> at the CAM-B3LYP<sup>37</sup>/6-31+G-(d,p)<sup>38-41</sup> level with a polarizable continuum model (PCM)<sup>42</sup> in MeOH. The optimized conformers were subsequently verified by frequency calculations at the same level. The geometries of all conformers close in energy were checked for redundancy. For ECD prediction, time-dependent density functional theory (TDDFT)<sup>43,44</sup> was conducted at the CAM-B3LYP<sup>37,45</sup> def2-TZVP<sup>46</sup> level to calculate the electronic excitation energies and rotational strengths with PCM in MeOH. Boltzmann-weighted ECD spectra were observed, where conformers with >1% Boltzmann population were calculated using SpecDis<sup>18</sup> for comparison by similarity factor with the experimentally determined data recorded in MeOH. The most up-to-date version (as of December 2021) of Multiwfn<sup>19</sup> software was used for visualization of molecular orbitals (isovalue = 0.03) involved in UV and ECD transitions.

## ■ ASSOCIATED CONTENT

### Supporting Information

The Supporting Information is available free of charge at <https://pubs.acs.org/doi/10.1021/acs.jnatprod.2c00861>.

IR, HRMS, and NMR spectra of compounds **1a–7**, **8a**, **9**, **10**, **13–15**, **17**, and **21** (PDF)

## ■ AUTHOR INFORMATION

### Corresponding Author

Leng Chee Chang – Department of Pharmaceutical Sciences, Daniel K. Inouye College of Pharmacy, University of Hawai'i at Hilo, Hilo, Hawaii 96720, United States; [orcid.org/0000-0001-9918-5612](https://orcid.org/0000-0001-9918-5612); Phone: +1 (808) 932-8124; Email: [lengchee@hawaii.edu](mailto:lengchee@hawaii.edu); Fax: +1 (808) 933-2974

### Authors

Feifei Liu – School of Life Sciences, Jiangsu Normal University, Xuzhou, Jiangsu 221116, People's Republic of China; Department of Pharmaceutical Sciences, Daniel K. Inouye College of Pharmacy, University of Hawai'i at Hilo, Hilo, Hawaii 96720, United States

Timothy J. O'Donnell – Department of Chemistry, University of Hawai'i at Manoa, Honolulu, Hawaii 96822, United States

Eun-Jung Park – Department of Pharmaceutical Sciences, Daniel K. Inouye College of Pharmacy, University of Hawai'i at Hilo, Hilo, Hawaii 96720, United States; Arnold and Marine Schwartz College of Pharmacy and Health Sciences, Long Island University, Brooklyn, New York 11201, United States; [orcid.org/0000-0001-9486-8692](https://orcid.org/0000-0001-9486-8692)

Sasha Kovacs – Department of Pharmaceutical Sciences, Daniel K. Inouye College of Pharmacy, University of Hawai'i at Hilo, Hilo, Hawaii 96720, United States

Kenzo Nakamura – Department of Pharmaceutical Sciences, Daniel K. Inouye College of Pharmacy, University of Hawai'i at Hilo, Hilo, Hawaii 96720, United States

Asim Dave – Arnold and Marine Schwartz College of Pharmacy and Health Sciences, Long Island University, Brooklyn, New York 11201, United States

Yuheng Luo – Department of Chemistry, University of Hawai'i at Manoa, Honolulu, Hawaii 96822, United States; [orcid.org/0000-0002-3124-1179](https://orcid.org/0000-0002-3124-1179)

Rui Sun – Department of Chemistry, University of Hawai'i at Manoa, Honolulu, Hawaii 96822, United States; [orcid.org/0000-0003-0638-1353](https://orcid.org/0000-0003-0638-1353)

Marisa Wall – Daniel K. Inouye U.S. Pacific Basin Agricultural Research Center, USDA-ARS, Hilo, Hawaii 96720, United States

Supakit Wongwiwatthananukit – Department of Pharmacy Practice, Daniel K. Inouye College of Pharmacy, University of Hawai'i at Hilo, Hilo, Hawaii 96720, United States

Dane Kaohelani Silva – Hale Ola Pono, LLC, Keaau, Hawaii 96749, United States

Philip G. Williams – Department of Chemistry, University of Hawai'i at Manoa, Honolulu, Hawaii 96822, United States; [orcid.org/0000-0001-8987-0683](https://orcid.org/0000-0001-8987-0683)

John M. Pezzuto – Department of Pharmaceutical Sciences, Daniel K. Inouye College of Pharmacy, University of Hawai'i at Hilo, Hilo, Hawaii 96720, United States; College of Pharmacy and Health Sciences, Western New England University, Springfield, Massachusetts 10119, United States

Complete contact information is available at:

<https://pubs.acs.org/10.1021/acs.jnatprod.2c00861>

### Author Contributions

T.J.O.D. and E.-J.P. contributed equally to this work.

### Notes

The authors declare no competing financial interest.

## ACKNOWLEDGMENTS

The authors specifically acknowledge Dr. Thomas F. Spande for proofreading the manuscript and for his scientific editing. This research was funded by the United States Department of Agriculture (USDA) Extramural Agreement (No. NACA 58-2040-5-012). The research project was supported by the National Natural Science Foundation of China (No. 31900293). We thank the Daniel K. Inouye College of Pharmacy for the research facility of the Mass Spectrometry and NMR Facility used in this study. We thank the advanced computing resources provided by the University of Hawaii Information Technology Service Cyberinfrastructure.

## REFERENCES

- (1) Nathan, C. *Nature* **2002**, *420*, 846–852.
- (2) Woolbright, B. L.; Jaeschke, H. *J. Hepatol.* **2017**, *66*, 836–848.
- (3) Fatkhullina, A. R.; Peshkova, I. O.; Koltsova, E. K. *Biochemistry* **2016**, *81*, 1358–1370.
- (4) Dinarello, C. A. *Cell* **2010**, *140*, 935–950.
- (5) Zongo, F.; Ribuot, C.; Boumendjel, A.; Guissou, I. *J. Ethnopharmacol.* **2013**, *148*, 14–26.
- (6) Laczko, R.; Chang, A.; Watanabe, L.; Petelo, M.; Csiszar, K. *Inflammopharmacology* **2020**, *28*, 525–540.
- (7) Saunders, J. G. *Bonplandia* **2007**, *16*, 143–180.
- (8) Cretton, S.; Dorsaz, S.; Azzollini, A.; Favre-Godal, Q.; Marcourt, L.; Ebrahimi, S. N.; Voinesco, F.; Michellod, E.; Sanglard, D.; Gindro, K. *J. Nat. Prod.* **2016**, *79*, 300–307.
- (9) Cretton, S.; Breant, L.; Pourrez, L.; Ambuehl, C.; Marcourt, L.; Ebrahimi, S. N.; Hamburger, M.; Perozzo, R.; Karimou, S.; Kaiser, M.; Cuendet, M.; Christen, P. *J. Nat. Prod.* **2014**, *77*, 2304–2311.
- (10) Bringmann, G.; Schlauer, J.; Rischer, H.; Wohlfarth, M.; Muhlbacher, J.; Buske, A.; Porzel, A.; Schmidt, J.; Adam, G. *Tetrahedron* **2000**, *56*, 3691–3695.
- (11) Buske, A.; Schmidt, J.; Hoffmann, P. *Phytochemistry* **2002**, *60*, 489–496.
- (12) Hoelzel, S.; Vieira, E. R.; Giacomelli, S. R.; Dalcol, I. I.; Morel, A. F. *Phytochemistry* **2005**, *66*, 1163–1167.
- (13) Jang, J. Y.; Dang, Q. L.; Choi, Y. H.; Choi, G. J.; Jang, K. S.; Cha, B.; Luu, N. H.; Kim, J.-C. *J. Agric. Food Chem.* **2015**, *63*, 68–74.
- (14) Jadulco, R. C.; Pond, C. D.; Wagoner, R. V.; Koch, M.; Gideon, O. G.; Matainaho, T. K.; Piskaut, P.; Barrows, L. R. *J. Nat. Prod.* **2014**, *77*, 183–187.
- (15) Maldaner, G.; Marangon, P.; Ilha, V.; Caro, M. S. B.; Burrow, R. A.; Dalcol, I. I.; Morel, A. F. *Phytochemistry* **2011**, *72*, 804–809.
- (16) Monteillier, A.; Cretton, S.; Ciclet, O.; Marcourt, L.; Ebrahimi, S. N.; Christen, P.; Cuendet, M. *J. Ethnopharmacol.* **2017**, *203*, 214–225.
- (17) Oliveira, P. L. D.; Tanaka, C. M. A.; Kato, L.; Silva, C. C. D.; Medina, R. P.; Moraes, A. P.; Sabino, J. R.; Oliveira, C. I. M. A. d. *J. Nat. Prod.* **2009**, *72*, 1195–1197.
- (18) Bruhn, T.; Schaumlöffel, A.; Hemberger, Y.; Pescitelli, G. *SpecDis version 1.71*, Berlin, Germany, 2017.
- (19) Tian, L.; Chen, F. *J. Comput. Chem.* **2012**, *33*, 580–592.
- (20) Cretton, S.; Kaiser, M.; Karimou, S.; Ebrahimi, S. N.; Mäser, P.; Breant, L.; Pourrez, L.; Cuendet, M.; Christen, P. *J. Nat. Prod.* **2020**, *83*, 3363–3371.
- (21) Zhu, F.; Du, B.; Xu, B. *Crit. Rev. Food Sci. Nutr.* **2018**, *58*, 1260–1270.
- (22) Han, B. H.; Lee, Y. J.; Yoon, J. J. *Eur. J. Integr. Med.* **2017**, *2017*, 326–336.
- (23) Jin, W.; Jia, Y.; Huang, L.; Wang, T.; Wang, H.; Dong, Y.; Zhang, H.; Fan, M.; Lv, P. *Pharmacol., Biochem. Behav.* **2014**, *124*, 145–152.
- (24) Marcu, K. B.; Otero, M.; Olivotto, E.; Borzi, R. M.; Goldring, M. B. *Curr. Drug Targets* **2010**, *11*, 599–613.
- (25) Youn, U. J.; Park, E. J.; Kondratyuk, T. P.; Sripisut, T.; Laphookhieo, S.; Pezzuto, J. M.; Chang, L. C. *Fitoterapia* **2016**, *114*, 92–97.
- (26) Vincent, J. L.; Zhang, H.; Szabo, C.; Preiser, J. C. *Am. J. Respir. Crit. Care Med.* **2000**, *161*, 1781–1785.
- (27) Kim, H. P.; Son, K. H.; Chang, H. W.; Kang, S. S. *J. Pharmacol. Sci.* **2004**, *96*, 229–245.
- (28) Rainsford, K. D. *Subcell. Biochem.* **2007**, *42*, 3–27.
- (29) Nicolin, V.; Ponti, C.; Narducci, P.; Grill, V.; Bortol, R.; Zweyer, M.; Vaccarezza, M.; Zauli, G. *Anat. Rec., Part A* **2005**, *286*, 945–954.
- (30) Park, E.-J.; Cheenpracha, S.; Chang, L. C.; Kondratyuk, T. P.; Pezzuto, J. M. *Nutr. Cancer* **2011**, *63*, 971–982.
- (31) Livak, K. J.; Schmittgen, T. D. *Methods* **2001**, *25*, 402–408.
- (32) Kondratyuk, T. P.; Park, E.-J.; Yu, R.; Breemen, R. B. v.; Asolkar, R. N.; Murphy, B. T.; Fenical, W.; Pezzuto, J. M. *Mar. Drugs* **2012**, *10*, 451–464.
- (33) Li, Z. Q.; Scheraga, H. A. *Proc. Natl. Acad. Sci. U. S. A.* **1987**, *84*, 6611–6615.
- (34) Kaminski, G. A.; Friesner, R. A.; Tirado-Rives, J.; Jorgensen, W. L. *J. Phys. Chem. B* **2001**, *105*, 6474–6487.
- (35) Schrödinger Release 2020-4: *MacroModel*, S.; Schrödinger LLC: New York, NY, 2020.
- (36) Frisch, M. J.; Trucks, G. W.; Schlegel, H. B.; Scuseria, G. E.; Robb, M. A.; Cheeseman, J. R.; Scalmani, G.; Barone, V.; Mennucci, B.; Petersson, G. A.; Nakatsuji, H.; Caricato, M.; Li, X.; Hratchian, H. P.; Izmaylov, A. F.; Bloino, J.; Zheng, G.; Sonnenberg, J. L.; Hada, M.; Ehara, M.; Toyota, K.; Fukuda, R.; Hasegawa, J.; Ishida, M.; Nakajima, T.; Honda, Y.; Kitao, O.; Nakai, H.; Vreven, T.; Montgomery, J. A.; Peralta, J. E.; Ogliaro, F.; Bearpark, M.; Heyd, J. J.; Brothers, E.; Kudin, K. N.; Staroverov, V. N.; Kobayashi, R.; Normand, J.; Raghavachari, K.; Rendell, A.; Burant, J. C.; Iyengar, S. S.; Tomasi, J.; Cossi, M.; Rega, N.; Millam, J. M.; Klene, M.; Knox, J. E.; Cross, J. B.; Bakken, V.; Adamo, C.; Jaramillo, J.; Gomperts, R.; Stratmann, R. E.; Yazyev, O.; Austin, A. J.; Cammi, R.; Pomelli, C.; Ochterski, J. W.; Martin, R. L.; Morokuma, K.; Zakrzewski, V. G.; Voth, G. A. S. P.; Dannenberg, J. J.; Dapprich, S.; Daniels, A. D.; Farkas, Foresman, J. B.; Ortiz, J. V. C. J.; Fox, D. J. *Gaussian 09*; Gaussian Inc., 2009.
- (37) Yanai, T.; Tew, D. P.; Handy, N. C. *Chem. Phys. Lett.* **2004**, *393*, 51–57.
- (38) Clark, T.; Chandrasekhar, J.; Spitznagel, G. W.; Schleyer, P. V. R. *J. Comput. Chem.* **1983**, *4*, 294–301.

- (39) Ditchfield, R.; Hehre, W. J.; Pople, J. A. *J. Chem. Phys.* **1971**, *54*, 724–728.
- (40) Hehre, W. J.; Ditchfield, R.; Pople, J. A. *J. Chem. Phys.* **1972**, *56*, 2257–2261.
- (41) Hariharan, P. C.; Pople, J. A. *Theor. Chim. Acta.* **1973**, *28*, 213–222.
- (42) Tomasi, J.; Mennucci, B.; Cammi, R. *Chem. Rev.* **2005**, *105*, 2999–3094.
- (43) Runge, E.; Gross, E. K. U. *Phys. Rev. Lett.* **1984**, *52*, 997–1000.
- (44) Gross, E. K. U.; Dobson, J. F.; Petersilka, M. *Top. Curr. Chem.* **1996**, *181*, 81–159.
- (45) Grauso, L.; Teta, R.; Esposito, G.; Menna, M.; Mangoni, A. *Nat. Prod. Rep.* **2019**, *36*, 1005–1030.
- (46) Weigend, F.; Ahlrichs, R. *Phys. Chem. Chem. Phys.* **2005**, *7*, 3297–3305.

## Recommended by ACS

### Bioactive Piperazic Acid-Bearing Cyclodepsipeptides, Lydiamycins E–H, from an Endophytic *Streptomyces* sp. Associated with *Cinnamomum cassia*

Weihong Wang, Heonjoong Kang, *et al.*

FEBRUARY 22, 2023  
JOURNAL OF NATURAL PRODUCTS

READ 

### Isolation of the Anti-Inflammatory Agent Myceliostatin from a Methionine-Enriched Culture of *Myceliophthora thermophila* ATCC 42464

Yanhua Wu, Kazuo Umezawa, *et al.*

FEBRUARY 03, 2023  
JOURNAL OF NATURAL PRODUCTS

READ 

### Noonindoles G–L: Indole Diterpene Glycosides from the Australian Marine-Derived Fungus *Aspergillus noonimiae* CMB-M0339

Sarani Kankanamge, Robert J. Capon, *et al.*

JANUARY 20, 2023  
JOURNAL OF NATURAL PRODUCTS

READ 

### Euphohelides A–C, *ent*-Abietane-Type Norditerpene Lactones from *Euphorbia helioscopia* and Their Anti-Inflammatory Activities

Hong-Ying Yang, Kun Gao, *et al.*

MARCH 01, 2023  
JOURNAL OF NATURAL PRODUCTS

READ 

Get More Suggestions >